

Modern Particle Detectors



Bernhard Ketzer

Helmholtz-Institut für Strahlen- und Kernphysik

SFB 1044 School 2016

Boppard

- Overview: old and new detectors
- Detection principles
- Interaction of charged particles with matter
 - **Inelastic collisions** with atomic electrons \Rightarrow ionization energy loss
 - Emission of **Cherenkov radiation**
 - Emission of **Transition radiation**
 - \Rightarrow unified treatment in **PAI model**
 - Emission of **Bremsstrahlung**
- Mean energy loss: **Bethe** formula and friends
- Energy loss distributions (straggling functions): **Landau** et al.

1. Introduction
2. Interaction of charged particles with matter
3. Ionization detectors
4. Position measurement and tracking
5. Photon detection
6. Calorimetry
7. Detector systems

3 Ionization Detectors

3.1 Detection of Ionization

3.2 Charge Transport

3.3 Gas Amplification

3.4 Signal Formation

Principle: collection of electrons and ions (holes) produced in detector medium by ionizing radiation

Detector material:

- gas \Rightarrow fast collection of e^- and ions, e.g. Ne, Ar
- liquid \Rightarrow higher density, e.g. liquid Ar
- solid \Rightarrow higher density, self-supporting, e.g. semiconductor

Setup:

- vessel with two electrodes and thin entrance window
- filled with active medium \Rightarrow **creation** of electron-ion (hole) pairs
- electric field between anode and cathode
 - separation of e^- and ions (holes), **drift and diffusion**
 - **signal induction**
 - collection at anode/cathode

Field-free gas: quick thermalization of charge carriers in collisions

⇒ Maxwell distribution of velocities (thermal equilibrium):

$$F(c)dc = 4\pi n \left(\frac{m}{2\pi kT} \right)^{3/2} c e^{-mc^2/(2kT)} dc \quad \bar{c} = \sqrt{\frac{8kT}{\pi m}}$$

$$\bar{E}_{\text{kin}} \equiv \varepsilon = \frac{m}{2} \bar{c}^2 = \frac{3}{2} kT \quad \text{Definition of temperature}$$

Point-like charge cloud at $t=0$ ⇒ Distribution at time t ?

Ansatz: $\mathbf{J} = -D \nabla n$

\mathbf{J} = flux density
 ∇n = gradient of particle density
 D = diffusion coefficient

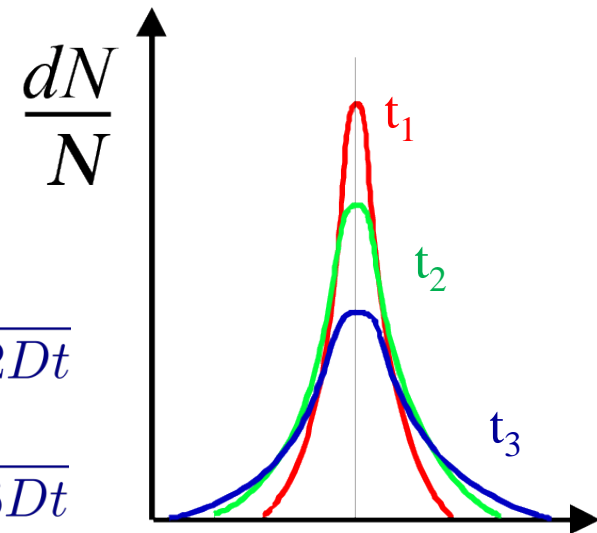
⇒ diffusion equation $\frac{\partial n}{\partial t} = D \Delta n$

Solution: Gaussian law

$$\frac{dN}{N} = \frac{ndz}{N} = \frac{1}{\sqrt{4\pi Dt}} e^{-z^2/4Dt} dz$$

$$\sqrt{\langle z^2 \rangle} \equiv \sigma_z = \sqrt{2Dt}$$

$$\sqrt{\langle r^2 \rangle} \equiv \sigma_r = \sqrt{6Dt}$$



Microscopically:

External electric field \Rightarrow acceleration

Collisions \Rightarrow slowing down

Macroscopically: drift motion with drift velocity u

Ansatz: Langevin equation

$$m \frac{du}{dt} = e\mathbf{E} + e(\mathbf{u} \times \mathbf{B}) - K\mathbf{u}$$

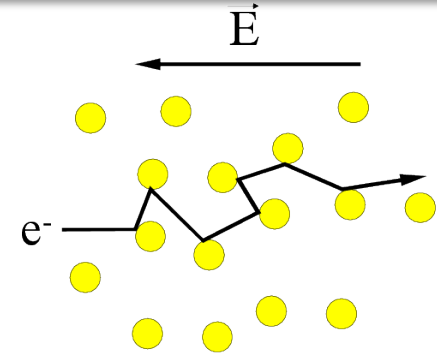
Ku = frictional force
 $\tau = \frac{m}{K}$ = characteristic time

Solution for $t \gg \tau$: steady state for which $\frac{du}{dt} = 0$

$$\mathbf{u} = \frac{e}{m} \tau |\mathbf{E}| \frac{1}{1 + \omega^2 \tau^2} \left[\hat{\mathbf{E}} + \omega \tau (\hat{\mathbf{E}} \times \hat{\mathbf{B}}) + \omega^2 \tau^2 (\hat{\mathbf{E}} \cdot \hat{\mathbf{B}}) \hat{\mathbf{B}} \right]$$

$\omega = \frac{eB}{m}$ = cyclotron frequency

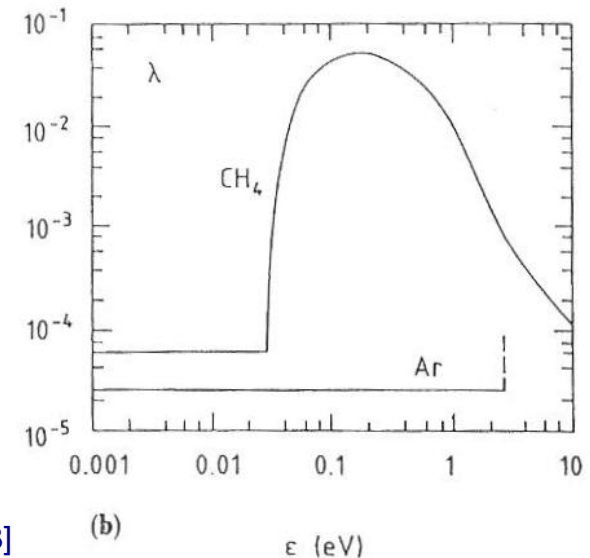
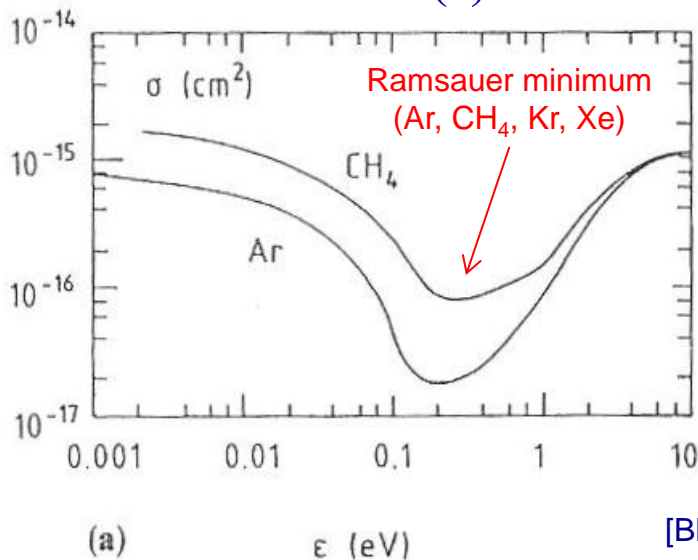
\Rightarrow Drift velocity u dominated by dimensionless parameter $\omega\tau$



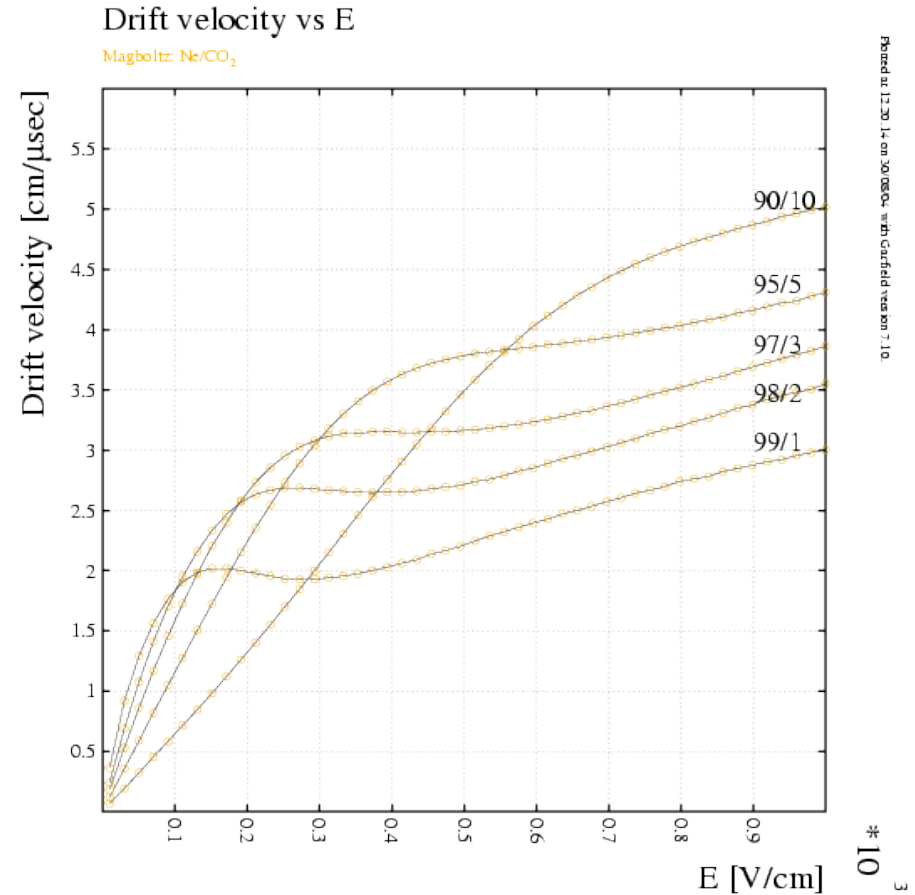
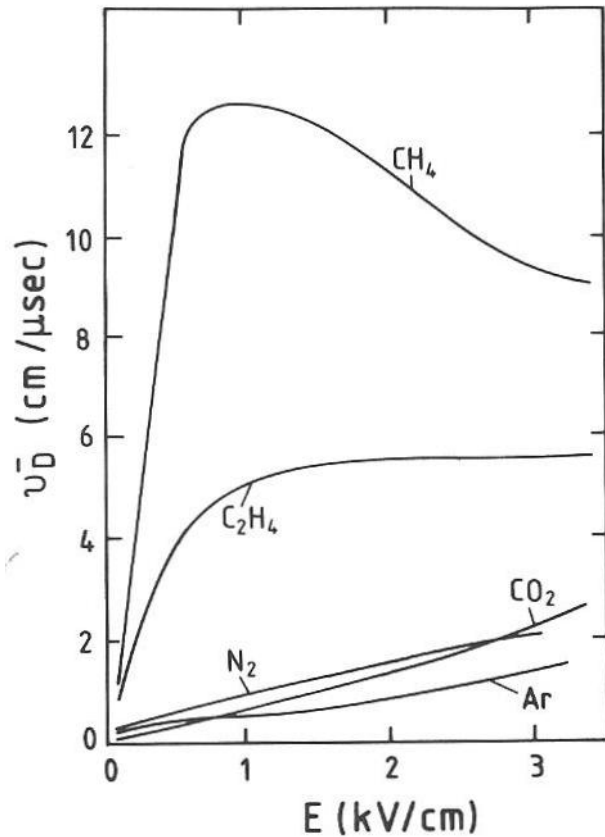
- rapid acceleration in electric field
- small energy loss in elastic collisions with atoms
- e^- momentum randomized in collisions
- energy gain in electric field is mainly in random motion \gg thermal energy

\Rightarrow drift velocity $u^2 = \frac{eE}{mn\sigma} \sqrt{\frac{\Lambda}{2}} \ll c^2 = \frac{eE}{mn\sigma} \sqrt{\frac{2}{\Lambda}}$ average velocity

$\Lambda = \Lambda(\epsilon)$ average fractional energy loss per collision
 $\sigma = \sigma(\epsilon)$ collision cross section



[Blum, Rolandi, Springer, 1993]



Ne/ CO_2 Mixtures

Printed at 12:20:14 on 30/08/04 with Garfield version 3.1.0

$\times 10^3$

Increase electric field in gaseous detector up to several kV/cm

⇒ electrons gain sufficient energy between collisions to ionize gas molecules

⇒ **avalanche generation**

Probability of ionization per unit path length: 1. Townsend coefficient

$$\alpha = \frac{1}{\lambda_{\text{ion}}} = n\sigma_{\text{ion}}$$

λ_{ion} = mean free path for sec. ionizing collision

σ_{ion} = cross section for ionizing collision

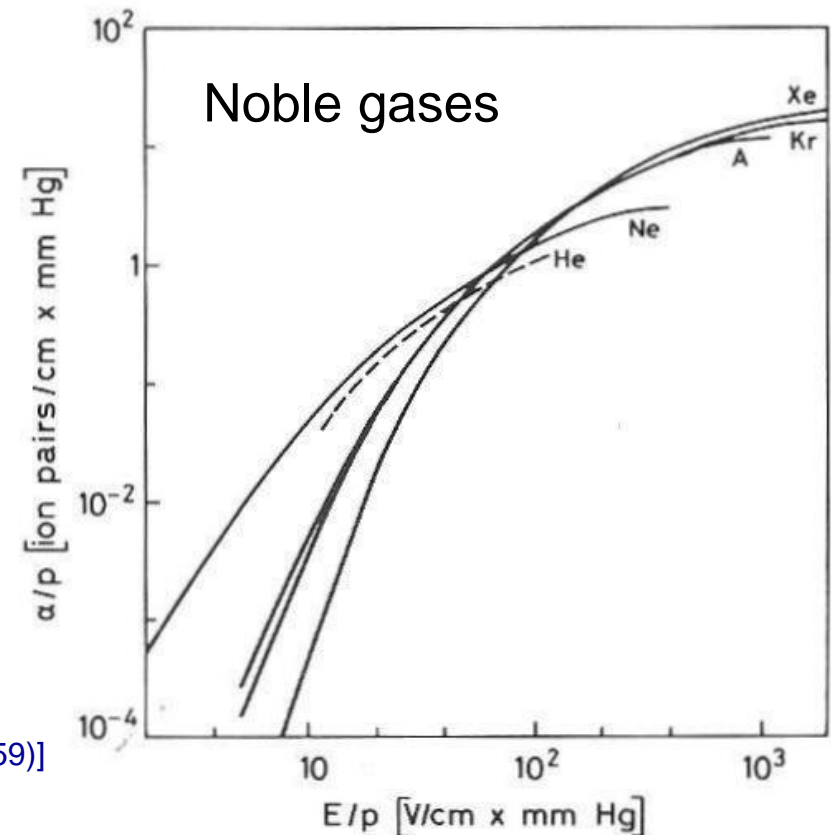
n = density of gas molecules

Homogeneous electric field:

$$dN = N\alpha dx \Rightarrow N = N_0 e^{\alpha x}$$

Gain: $G = \frac{N}{N_0} = e^{\alpha x}$

[S.C. Brown, Basic Data of Plasma Physics, MIT Press (1959)]



Proportional counter: average number of electrons \propto initial electrons N_i

Random nature of multiplication process \Rightarrow fluctuations

Assumption: each initiating electron develops its own small avalanche, independent of presence of other electrons nearby

$$N = n_1 + n_2 + n_3 + \dots + n_k$$

Probability distribution of number N of total electrons

= sum over probability distributions $P(n)$ of number of electrons n in individual small avalanches (mean \bar{n} , variance σ^2)

If number k of initiating electrons large \Rightarrow central limit theorem

$$F(N) = \frac{1}{S\sqrt{2\pi}} \exp[-(N - \bar{N})^2 / 2S^2] \quad \text{with} \quad \bar{N} = k\bar{n} \quad \text{and} \quad S^2 = k\sigma^2$$

- Exact shape of $P(n)$ not needed if k large
- Often: detection of **single electrons** important, e.g. drift chambers, PMT
 $\Rightarrow P(n)$ particularly interesting

Avalanche distribution in weak fields: Yule-Furry law

$$P(n, s) = \frac{1}{\bar{n}(s)} e^{-\frac{n}{\bar{n}(s)}} \quad \text{and} \quad \sigma(s) = \bar{n}(s) \quad (s = \text{drift coordinate})$$

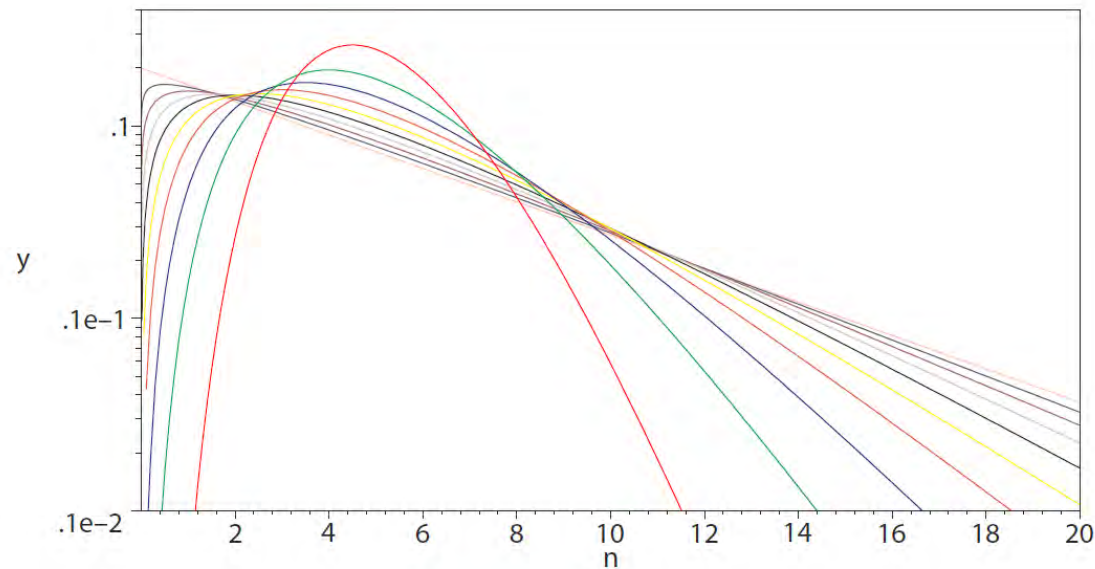
- i.e. a purely exponential distribution with small signals being most probable!
- R.m.s. width is equal to the mean

Avalanche distribution in strong fields:

- Different distributions in literature: Legler et al., ...
- Often used as good approximation: Polya distribution

$$P(n) = \frac{1}{b\bar{n}} \frac{1}{k!} \left(\frac{n}{b\bar{n}} \right)^k e^{-n/b\bar{n}}$$

$$k = \frac{1}{b} - 1$$



- $b=1 \Rightarrow$ Furry distribution (single exponential):
Probability for birth of new e^- prop. to n
- $b=0 \Rightarrow$ Poisson distribution: Prob. for birth of new e^- indep. of n



Assume statistically independent sources of fluctuations:

- k ionization electrons, $\langle k \rangle = N_i$, $\sigma_i = \sqrt{F \cdot N_i}$ (F Fano factor)
- each ionization electron creates an avalanche of size n_j ,

$$\langle n \rangle = \frac{1}{N_i} \sum_{j=1}^{N_i} n_j, \quad \sigma_{\bar{n}}^2 = \frac{1}{N_i} \sigma_n^2$$

⇒ signal amplitude

$$S = \sum_{j=1}^{N_i} n_j = N_i \cdot \bar{n}$$

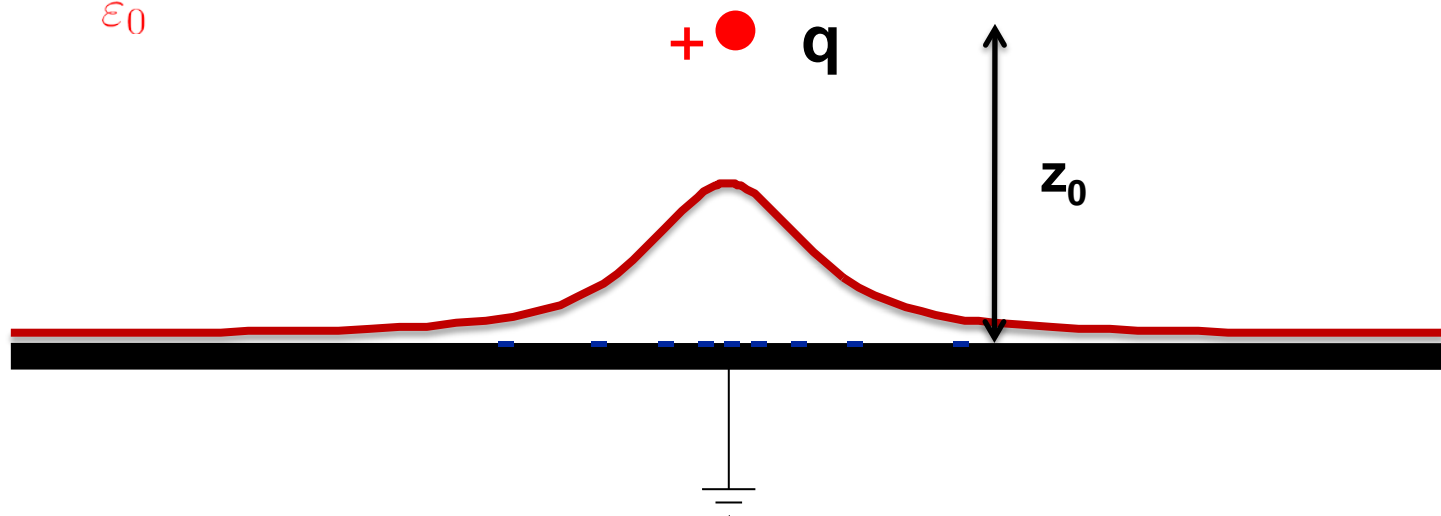
signal fluctuations

$$\left(\frac{\sigma_S}{S} \right)^2 = \left(\frac{\sigma_i}{N_i} \right)^2 + \left(\frac{\sigma_{\bar{n}}}{\bar{n}} \right)^2 = \left(\frac{\sigma_i}{N_i} \right)^2 + \frac{1}{N_i} \left(\frac{\sigma_n}{\bar{n}} \right)^2$$

Consider charge q above a grounded electrode

- electric field is perpendicular to conductor at the surface
- changes take place only on surface
- surface charge density σ and electric field E on the surface are related by Gauss' law

$$EA = \frac{1}{\epsilon_0} \sigma A \Rightarrow \sigma = \epsilon_0 E$$

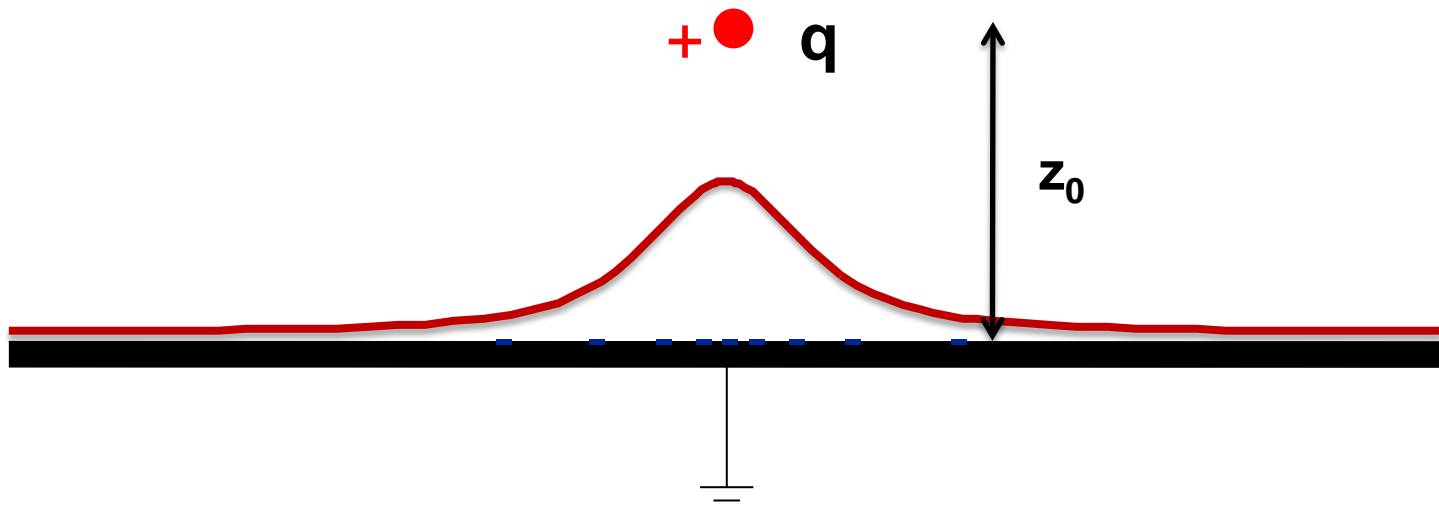


In order to find the charge induced on an electrode, we have to

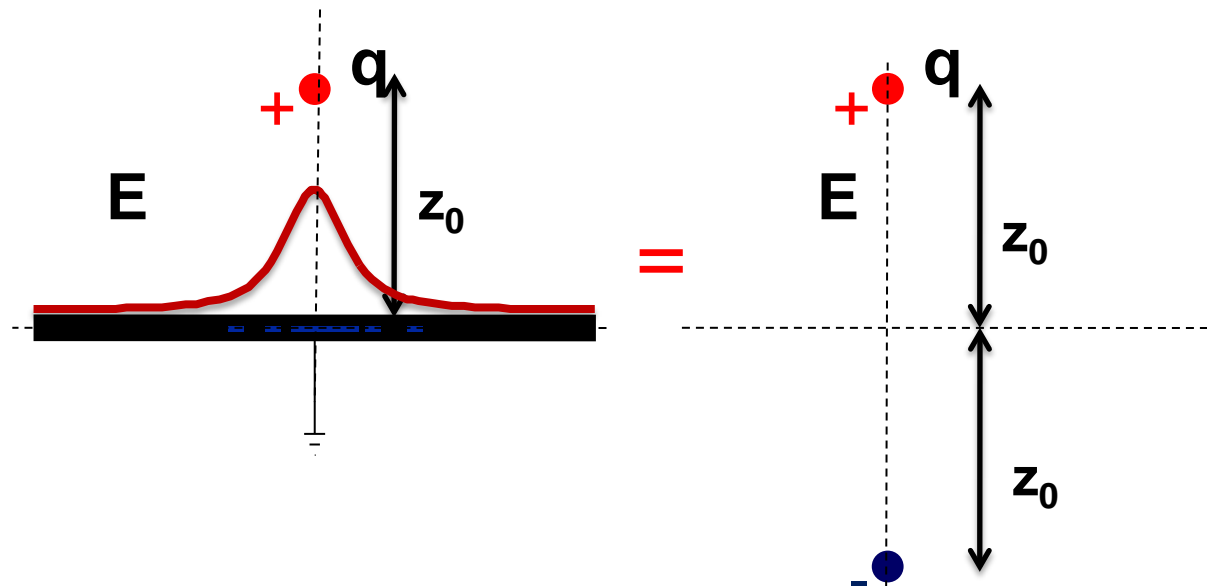
- a) solve the Poisson equation with boundary condition $\phi = 0$ on the conductor surface

$$\Delta\varphi = -\frac{\rho}{\varepsilon_0}, \quad \mathbf{E} = -\nabla\varphi$$

- b) calculate the electric field E on the surface of the conductor
- c) integrate $\varepsilon_0 E$ over the surface of the electrode

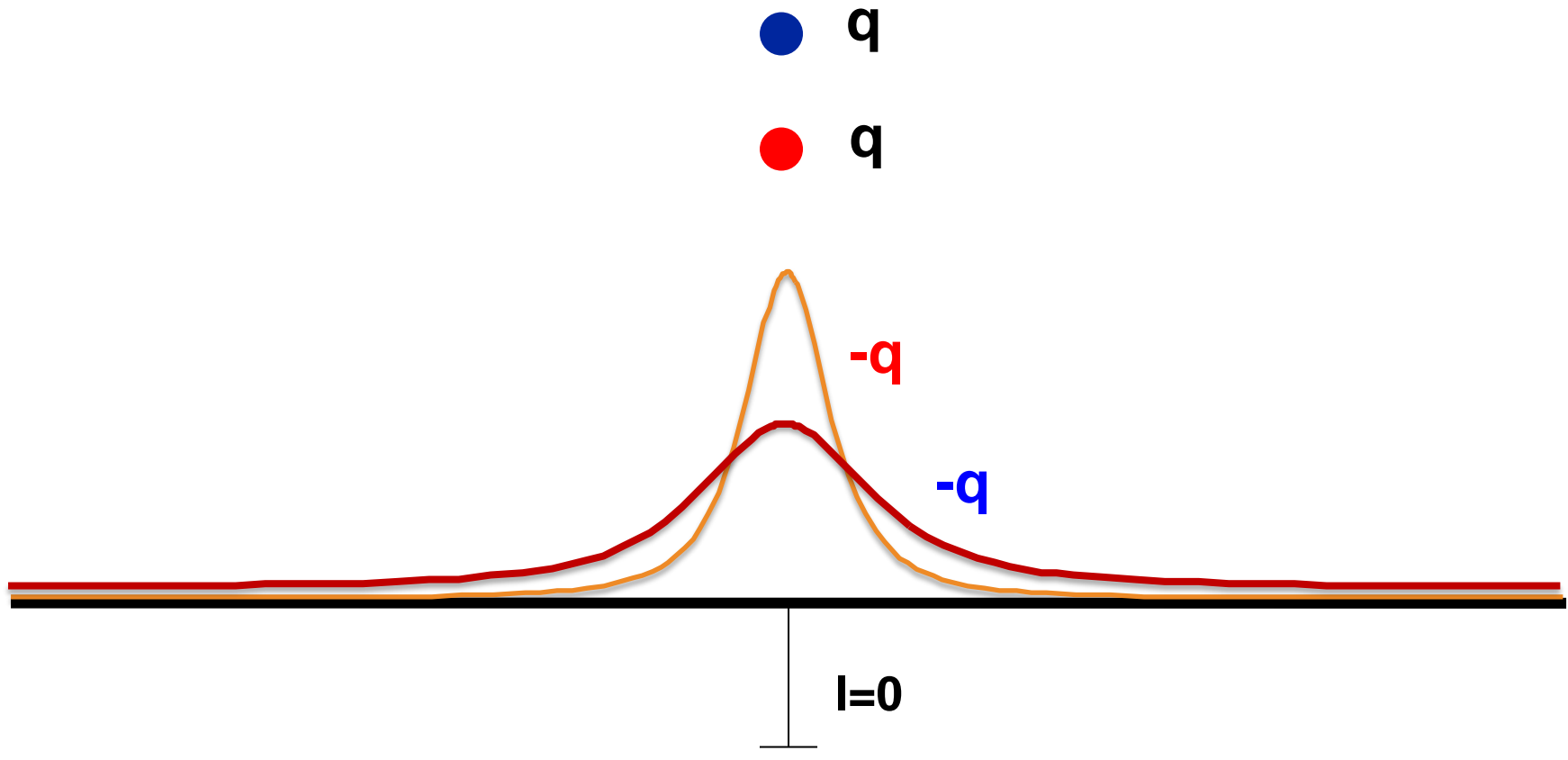


For this particularly simple setup with one electrode
 ⇒ use mirror charge



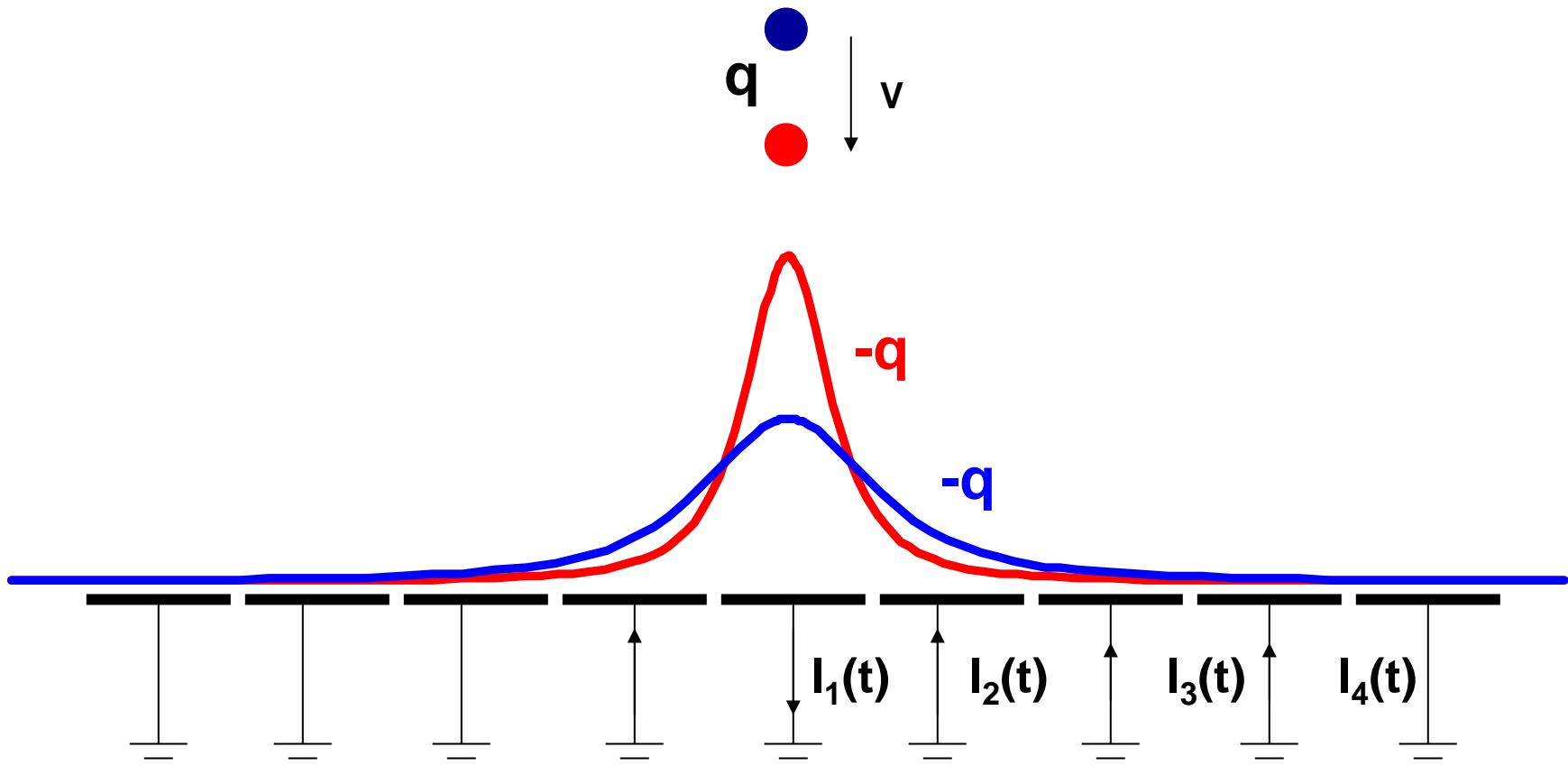
Movement of charge q (no external field needed!)

⇒ change of induced surface charge on electrode



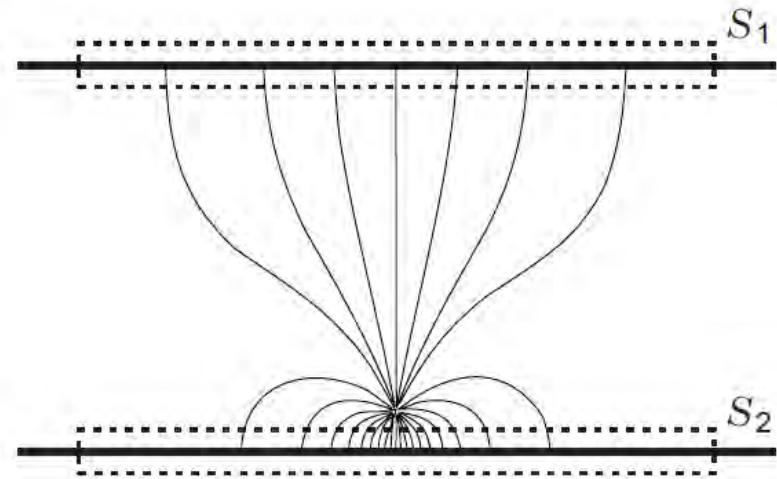
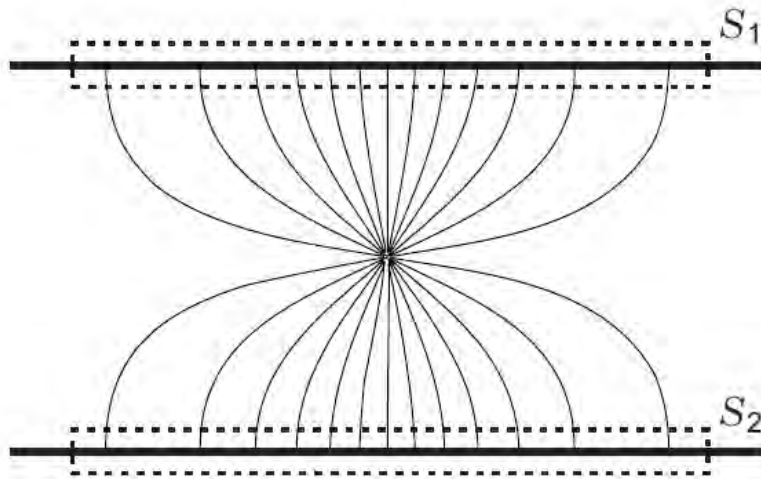
Movement of charge q (no external field needed!)

- ⇒ change of induced surface charge on electrode
- ⇒ current on segmented electrodes



How to calculate the induced signal?

- solve Poisson equation with moving charge
- use mirror charges to get rid of electrodes
- use Ramo-Shockley theorem



[H. Spieler, Semiconductor detector systems, Oxford, 2005]

[W. Shockley, J. Appl. Phys. 9, 635 (1938), S. Ramo, Proc. IRE 27, 584 (1939)]

Calculation of signals induced on grounded electrodes:

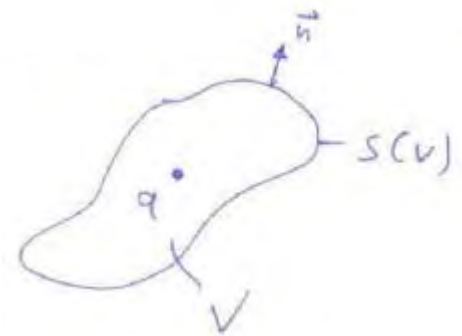
- Gauss' Law: point charge inside closed surface

$$\oint_V \mathbf{E} \cdot \mathbf{n} da = \frac{1}{\epsilon_0} \int_V \rho(\mathbf{x}) d^3x$$

- Green's 2nd theorem:

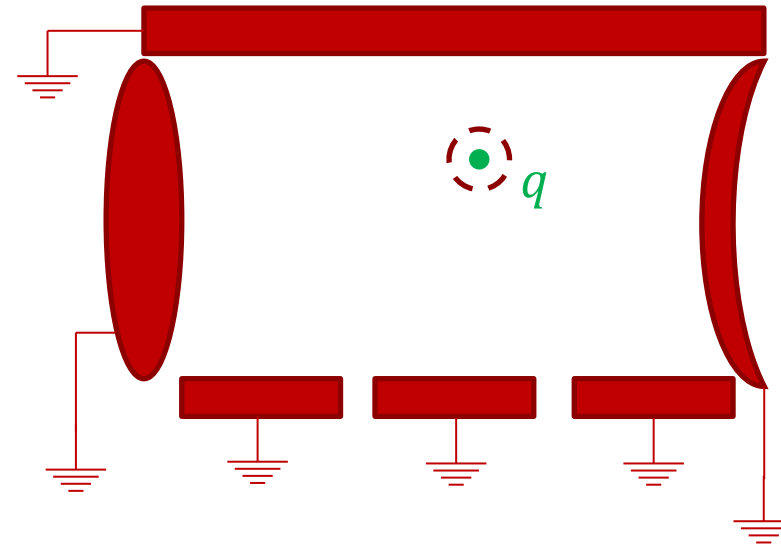
$$\int_V (\phi \Delta \psi - \psi \Delta \phi) d^3x = \oint_S \left(\phi \frac{\partial \psi}{\partial n} - \psi \frac{\partial \phi}{\partial n} \right) da$$

with $\frac{\partial \phi}{\partial n} \equiv \nabla \phi \cdot \mathbf{n} [= -\mathbf{E} \cdot \mathbf{n}]$



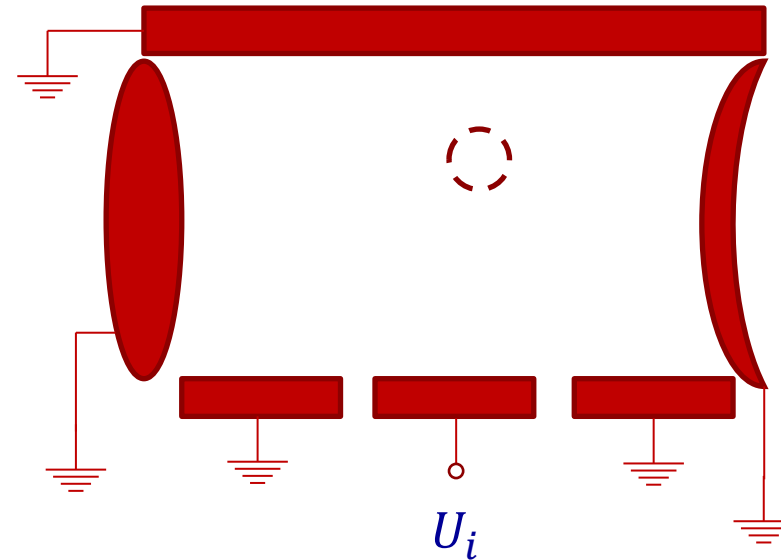
Consider detector volume delimited by grounded electrodes:

- Real situation: charge q at position x_0 ,
all electrodes grounded, i.e.
 $U_i = 0, i = 1, 2, \dots \Rightarrow$ solution $\phi(\mathbf{x})$



Consider detector volume delimited by grounded electrodes:

- Real situation: charge q at position \mathbf{x}_0 , all electrodes grounded, i.e.
 $U_i = 0, i = 1, 2, \dots \Rightarrow$ solution $\phi(\mathbf{x})$
- Auxiliary situations: charge q removed, all electrodes grounded except electrode i , i.e.
 $U_j = 0, j \neq i \Rightarrow$ solutions $\phi_i(\mathbf{x})$ with
 $\phi_i(\mathbf{x}) = U_i$ at surface of electrode i

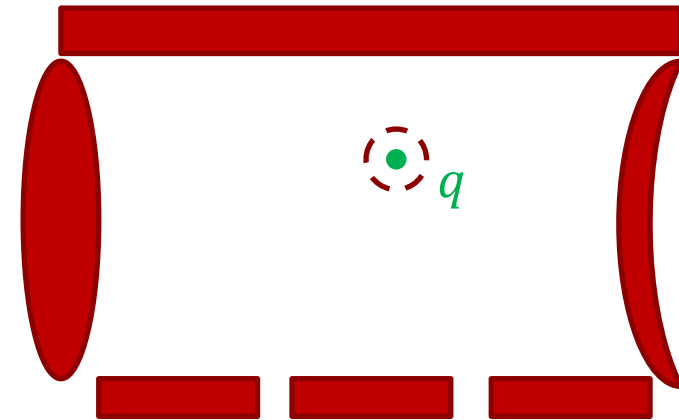


Space between electrodes and charge q free of charges

$$\Rightarrow \Delta\phi(\mathbf{x}) = 0$$

$$\Delta\phi_i(\mathbf{x}) = 0$$

Apply Green's 2nd theorem to volume V delimited by $S(V)$:



$$\underbrace{\int_V (\phi \Delta \phi_i - \phi_i \Delta \phi) d^3x}_{= 0} = \int_{S(V)} \left(\phi \frac{\partial \phi_i}{\partial n} - \phi_i \frac{\partial \phi}{\partial n} \right) da \quad \text{for every } i$$

Solve surface integral by splitting it up into 3 parts

$$\Rightarrow Q_i = -q \frac{\phi_i(\mathbf{x}_0)}{U_i}$$

induced charge on electrode i by charge q at position x_0 when all electrodes are grounded

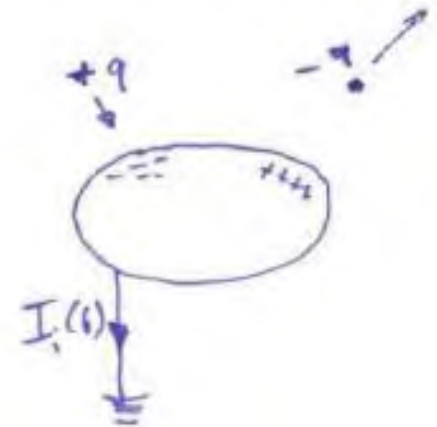
$\phi_i(x_0) =$ potential at point x_0 when point charge q is removed, electrode i is put to potential U_i and all other electrodes are grounded

weighting potential of electrode i

Point charge moving along trajectory $x_0(t)$

⇒ time-dependent induced charge on electrode i

⇒ current $I_i(t) = -\frac{dQ_i(t)}{dt}$



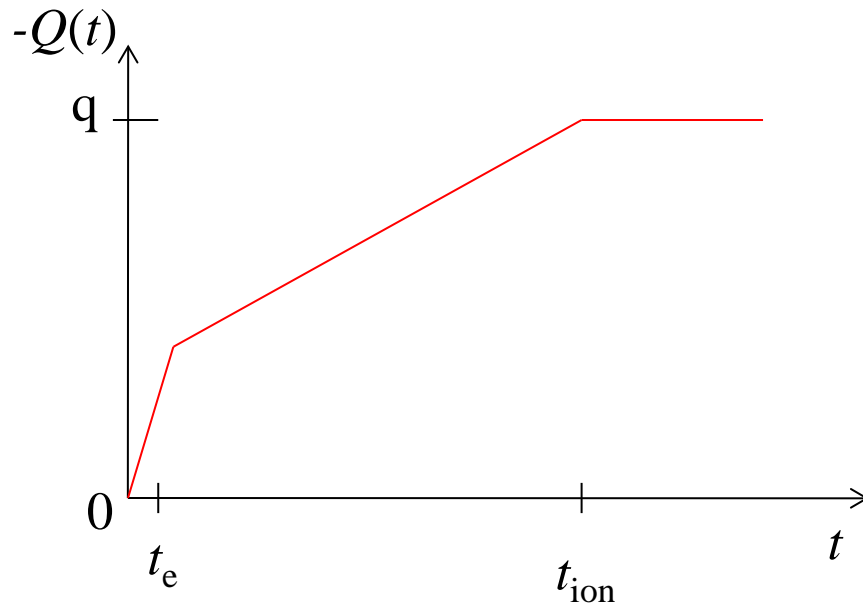
Sign convention: positive current points away from electrode

$$I_i(t) = -\frac{dQ_i(t)}{dt} = \frac{q}{U_i} \frac{d}{dt} \phi[\mathbf{x}_0(t)]$$

$$I_i(t) = \frac{q}{U_i} \nabla \phi_i[\mathbf{x}_0(t)] \cdot \frac{d\mathbf{x}_0(t)}{dt} = -\frac{q}{U_i} \mathbf{E}_i[\mathbf{x}_0(t)] \cdot \mathbf{v}(t)$$

Ramo-Shockley
Theorem

The current induced on a grounded electrode by a point charge q moving along a trajectory $\mathbf{x}_0(t)$ is $I_i(t)$, where $\mathbf{E}_i(\mathbf{x}_0)$ is the electric field in the case where the charge q is removed, electrode i is set to voltage U_i , and all other electrodes are grounded.



- Steep linear rise until e- reach anode
- Slow linear rise until ions reach cathode, contribution from e- constant
- Constant for $t > t_{ion}$

Example: Ar at NTP

$$d = 5 \text{ cm}$$

$$E = 500 \text{ V/cm}$$



$$\Rightarrow t_e = 12.5 \mu\text{s}$$

$$t_{ion} = 6 \text{ ms}$$



How do the real field and the weighting field look like?

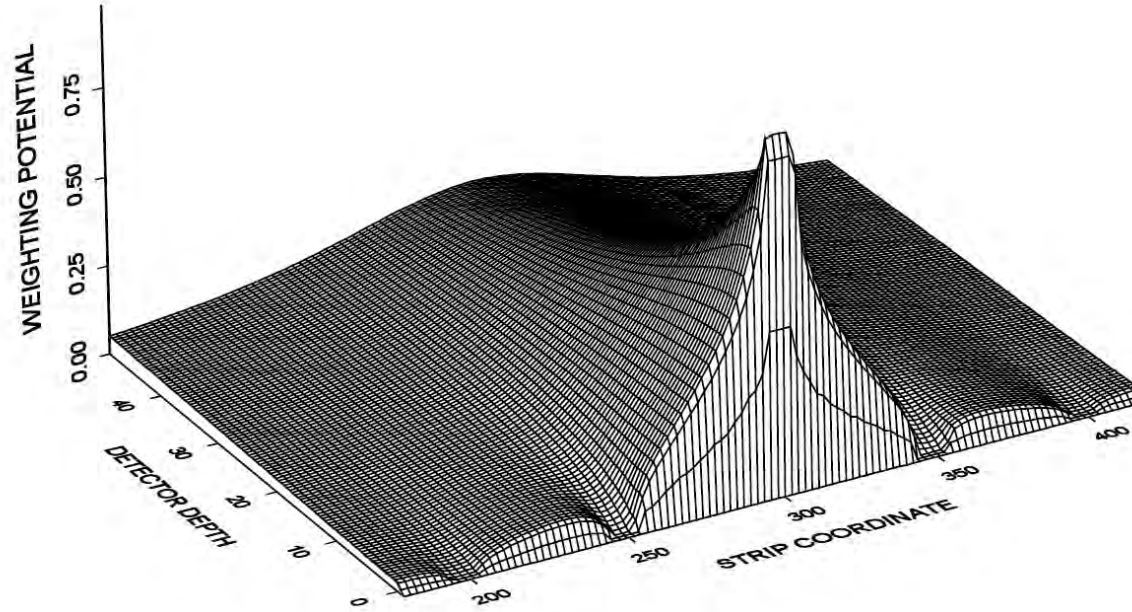
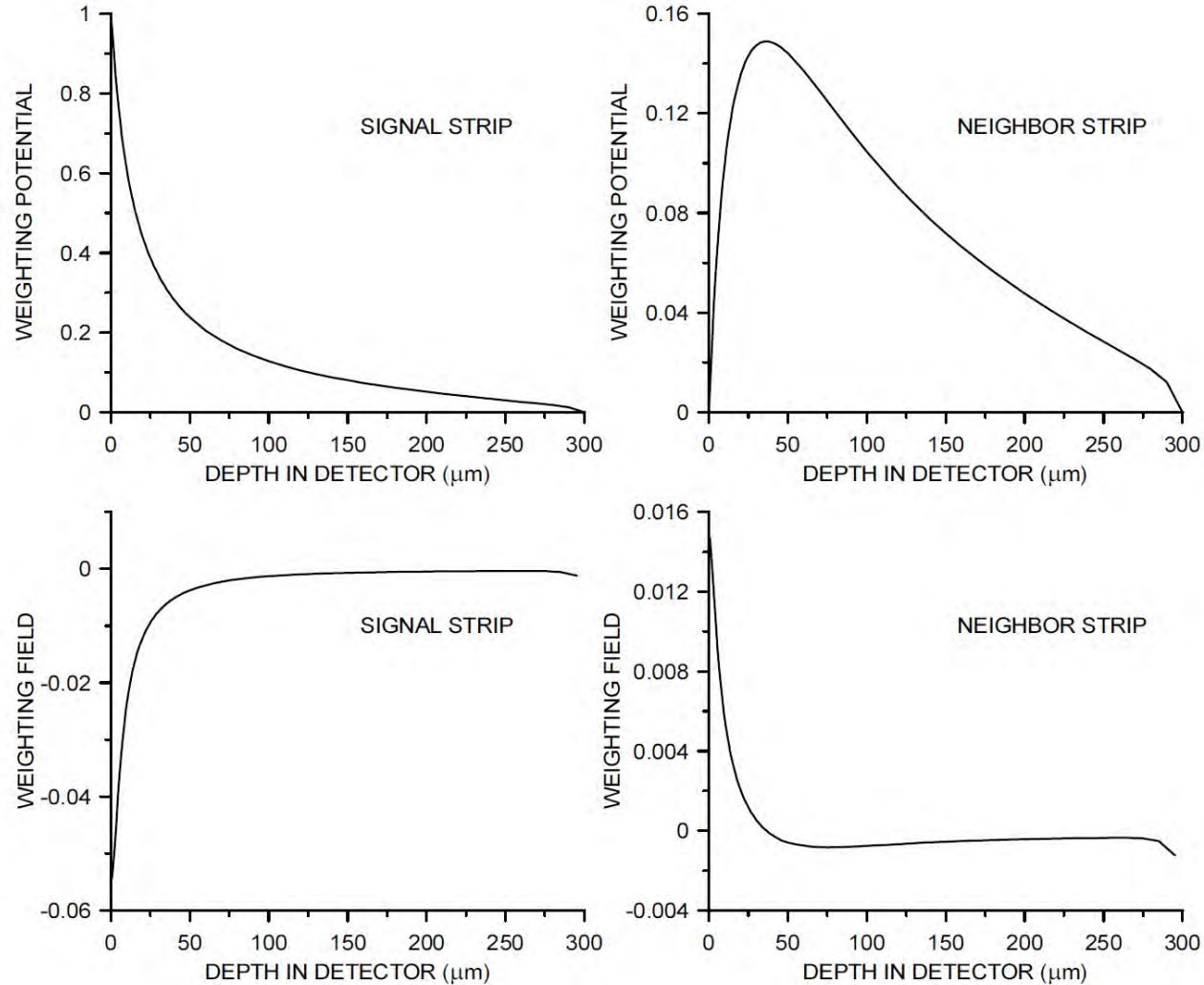
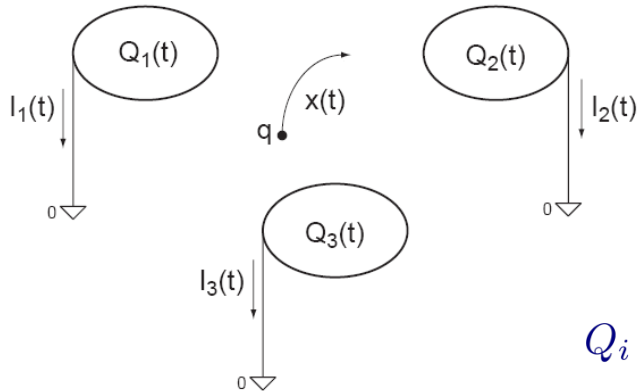


FIG. 2.29. Weighting potential for a $300 \mu\text{m}$ thick strip detector with strips on a pitch of $50 \mu\text{m}$. The central strip is at unit potential and the others at zero. Only $50 \mu\text{m}$ of depth are shown.

[H. Spieler, Semiconductor detector systems, Oxford, 2005]



[H. Spieler, Semiconductor detector systems, Oxford, 2005]

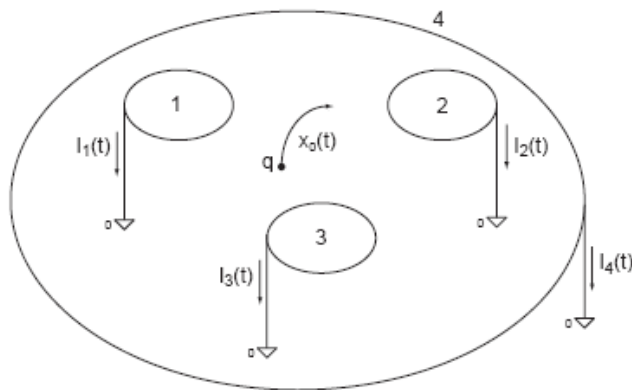


Consequences:

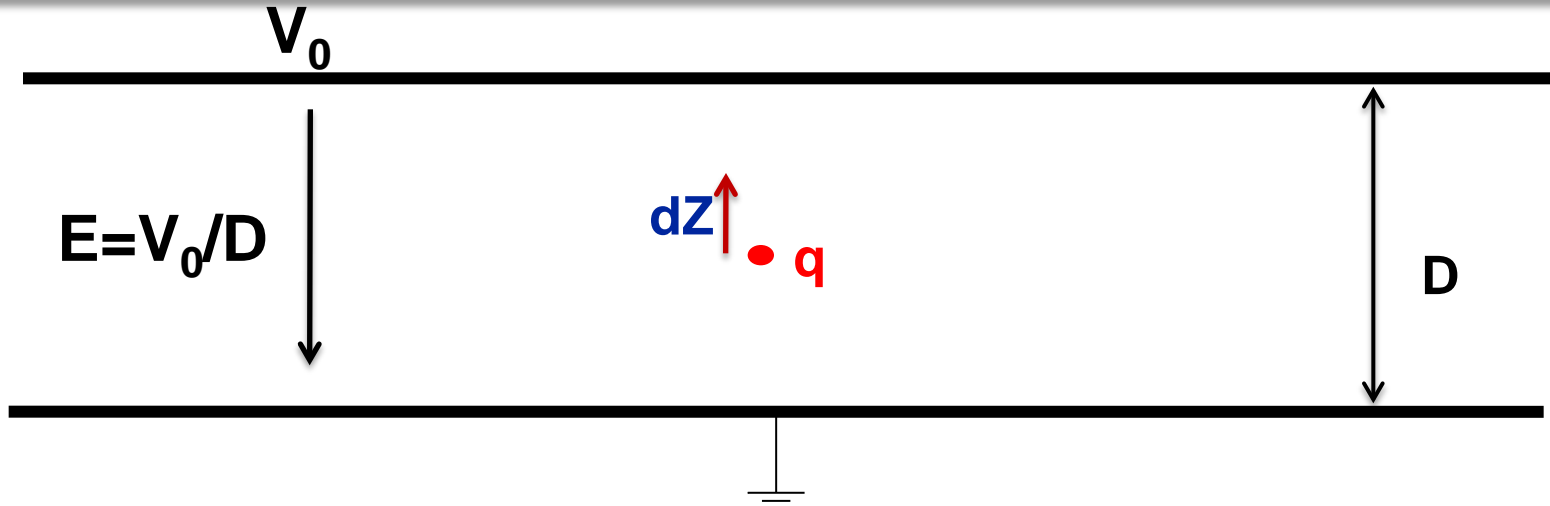
1. Charge induced on electrode i by a charge q moving from point 1 to 2 is

$$Q_i = \int_{t_1}^{t_2} I_i(t) dt = -\frac{q}{U_i} \int_{t_1}^{t_2} \mathbf{E}_i[\mathbf{x}(t)] \dot{\mathbf{x}}(t) dt = \frac{q}{U_i} [\phi_i(\mathbf{x}_1) - \phi_i(\mathbf{x}_2)]$$

and is independent of the actual path



2. Once all charges have arrived at the electrodes, the total induced charge in a given electrode is equal to the charge that has arrived at this electrode
3. In case there is one electrode enclosing all others, the sum of all induced currents is zero at any time



$$\text{Energy} = \frac{1}{2} C V_0^2 = \frac{1}{2} \frac{Q^2}{C}$$

$$dW = q E dz = \frac{q V_0}{D} dz$$

$$d(\text{Energy}) = dW$$

$$d \frac{1}{2} \frac{Q^2}{C} = \frac{q V_0}{D} dz$$

$$\frac{1}{2} \frac{1}{C} Q dQ = \frac{q V_0}{D} dz$$

$$dQ = \frac{q}{D} dz$$

Gives correct result!

see e.g. [W.R. Leo, Techniques for Nuclear and Particle Physics, Springer, 1987]

- Signal is calculated using energy balance:
 - Energy gained by charge in electric field =
 - change of energy stored in capacitor
- In some special cases, this argument gives the correct result, e.g. for a 2-electrode system because there the weighting field and the real field are equal.
- But the argument is very misleading:
 - An induced current signal has nothing to do with energy. In a gas detector the electrons are moving at constant speed in a constant electric field, so the energy gained by the electron in the electric field is lost into collisions with the gas, i.e. heating of the gas.
 - In absence of an electric field, the charge can be moved across the gap without using any force and currents are flowing.

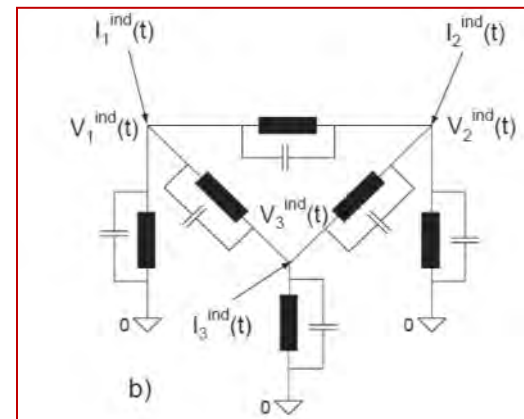
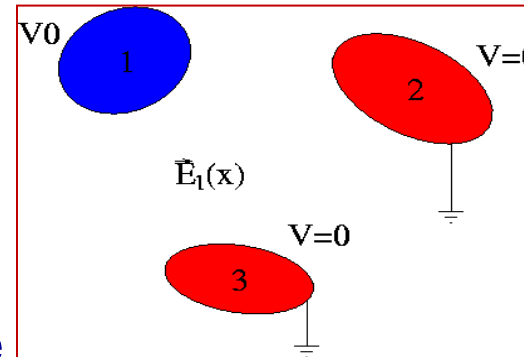
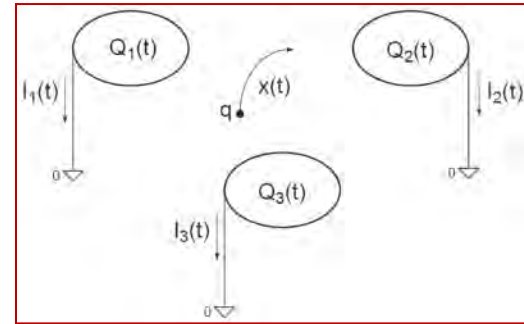
1. Calculate particle trajectory $x_0(t)$ in the „real“ electric field
2. Remove all impedance elements, ground the electrodes and calculate currents induced by moving charge on grounded electrodes

$$I_i(t) = \frac{q}{U_i} \nabla \phi_i [\mathbf{x}_0(t)] \cdot \frac{d\mathbf{x}_0(t)}{dt} = -\frac{q}{U_i} \mathbf{E}_i [\mathbf{x}_0(t)] \cdot \mathbf{v}(t)$$

3. Place these currents as ideal current sources on a circuit where the electrodes are simple nodes and the mutual electrode capacitances are added between the nodes. They are calculated from the weighting field by

$$c_{nm} = \frac{\varepsilon_0}{V_w} \oint_{A_n} \mathbf{E}_m(\mathbf{x}) dA$$

$$C_{nn} = \sum_m c_{nm} \quad C_{nm} = -c_{nm} \quad n \neq m$$



4 Position Measurement

4.1 Resistive Plate Chambers

4.2 Micropattern Gaseous Detectors

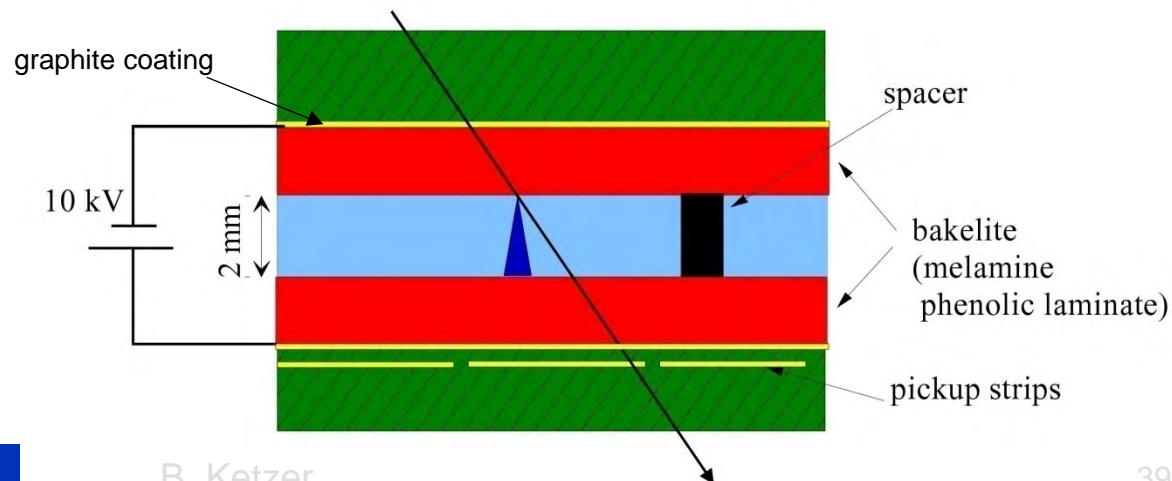
4.3 Semiconductor Detectors

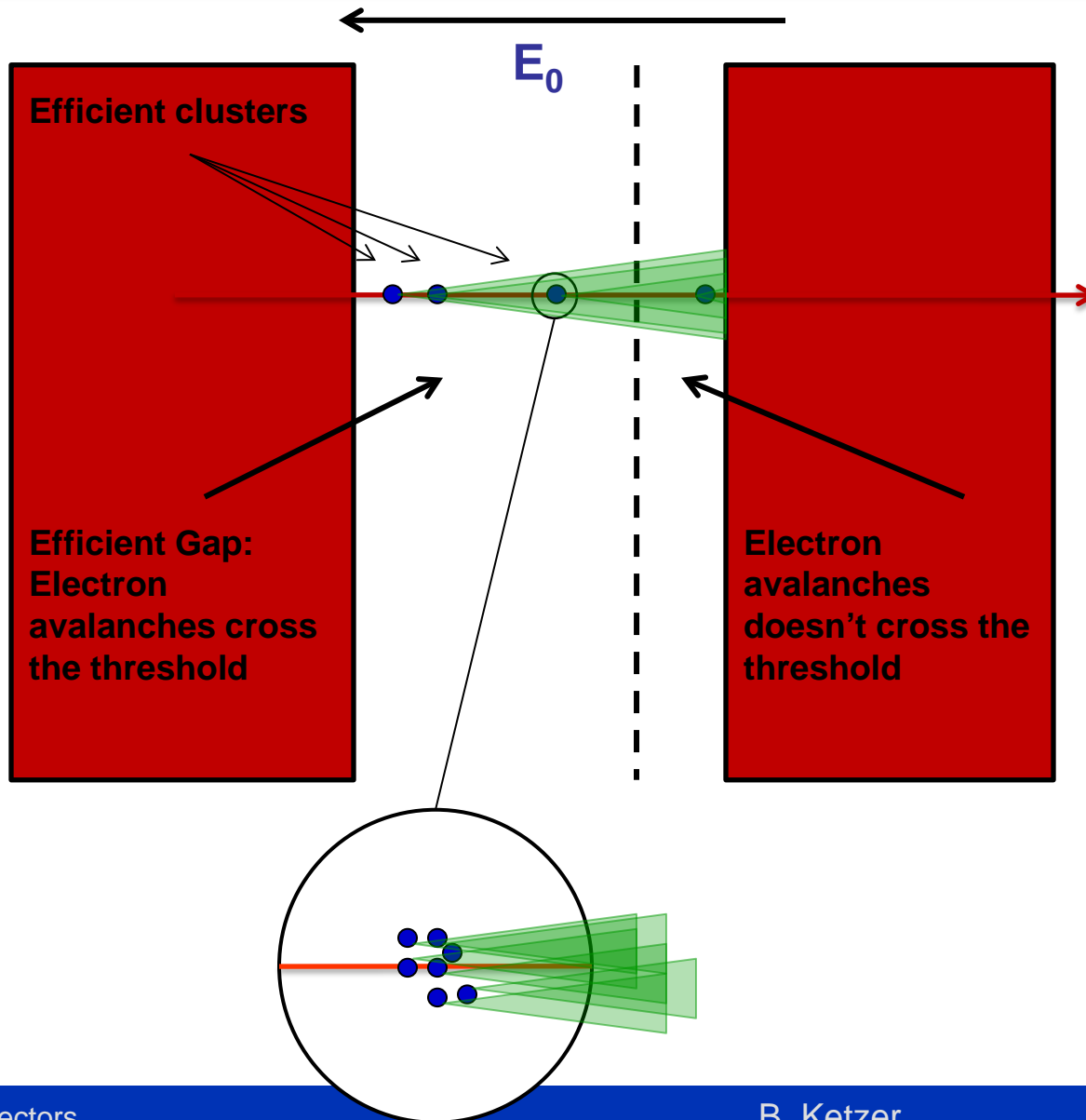
4.4 Track Reconstruction

Principle:

[R. Santonico et al., NIM 187, 377 (1981)]

- Parallel plate counter with strong uniform electric field: ~ 50 kV/cm, 2 mm gap
 - ⇒ very good time resolution: $\sigma_t < 1$ ns
 - instant avalanche multiplication for all primary clusters
 - dominated by avalanche statistics, not primary ionization statistics
- High-ohmic electrode material (glass: $\rho = 10^{12}$ Ωcm , Bakelite: 10^{10} - 10^{11} Ωcm)
 - ⇒ local decrease of electric field at position of avalanche
 - ⇒ blind spot for time $\tau \sim \rho\epsilon_0\epsilon_r$ (relaxation time, 10 ms – 1 s)
- Pickup strips for position information





Number of clusters per unit length follows strictly a Poisson distribution.

Number of efficient clusters follows to a good approximation the same Poisson distribution.

The number of electrons per cluster follows approximately a $1/n^2$ distribution.

→ Number of efficient electrons follows approximately a "Landau" distribution.

Each individual electron starts an avalanche, inducing a signal which will cross a given threshold of the readout electronics → time.

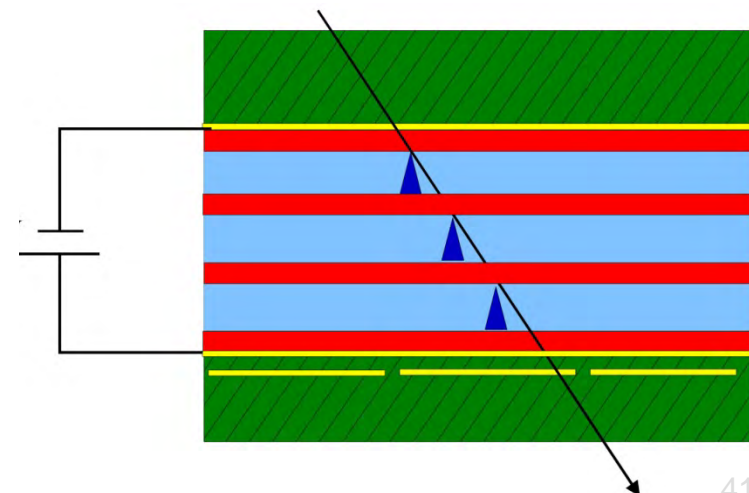
Operation:

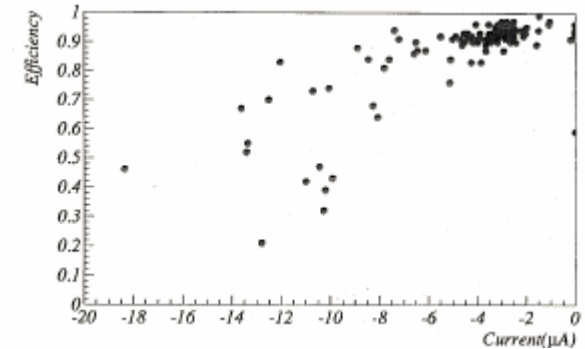
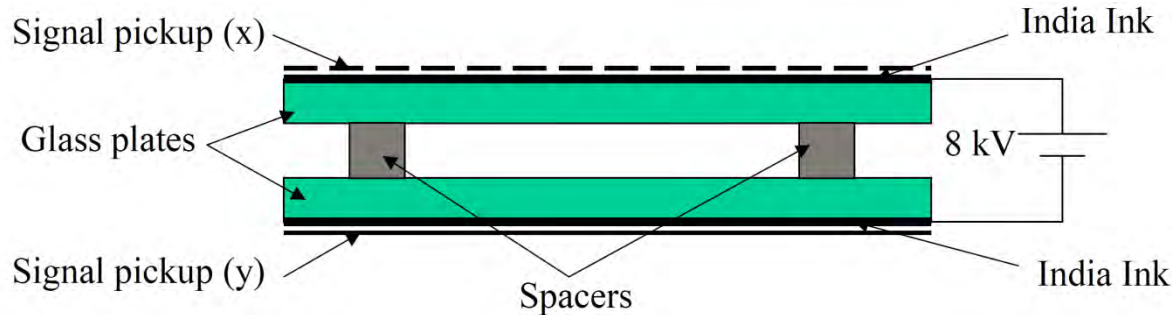
- **Streamer mode:** L3, BaBar, BELLE
 - large signals (up to $\sim nC$) \Rightarrow no amplifier needed
 - low rate capability: a few 100 Hz/cm²
- **Proportional mode:** ATLAS, CMS μ trigger
 - suppression of streamers by addition of small amounts of SF₆
 - higher rate capability: a few kHz/cm²
 - signal $\sim 10\times$ smaller \Rightarrow low-noise amplifier
 - less aging

Multi-gap RPC: ALICE TOF barrel, FOPI

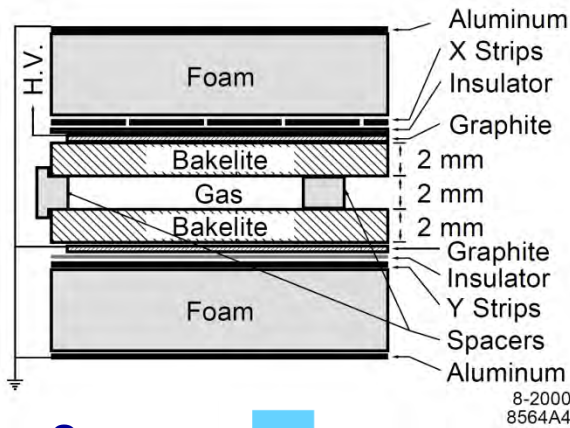
- 0.2 – 0.3 mm gaps
- \Rightarrow improved efficiency
- \Rightarrow improved time resolution (smaller gaps)

$$\sigma_t = 50 - 100 \text{ ps}$$



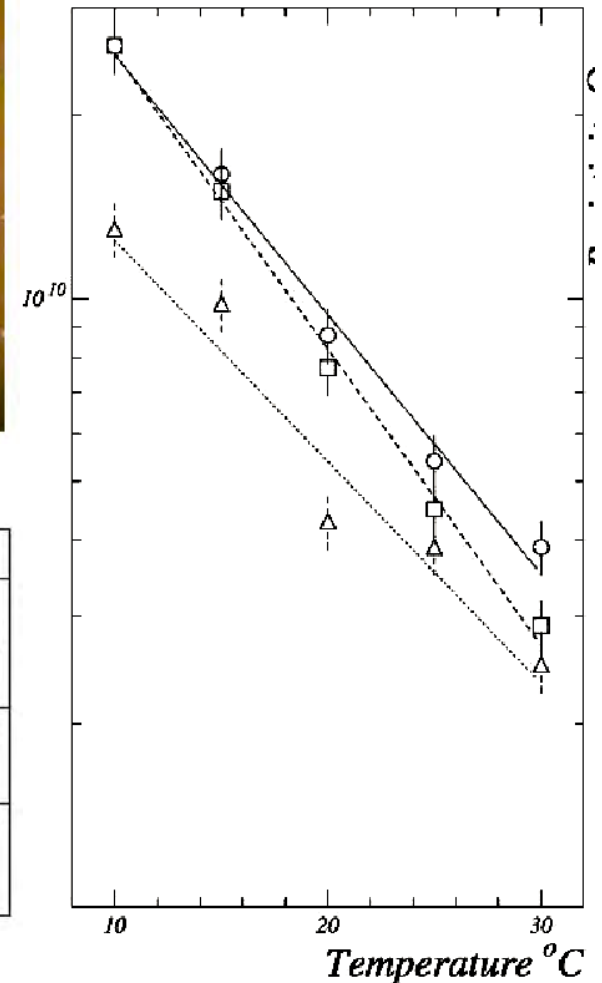


- Operation mode: streamer
- Material: float glass
- Observation: high dark currents, deterioration of efficiency
- Increase of voltage increases dark current \Rightarrow "RPC death spiral"
- Cause: water content $>$ 2000 ppm due to polyethylene tubing
- $C_2H_2F_4 + \text{water} \Rightarrow \text{HF acid}$, etched glass surface
- Solution: replace polyethylene by copper tubing



Spacer:

Conductive rubber technique

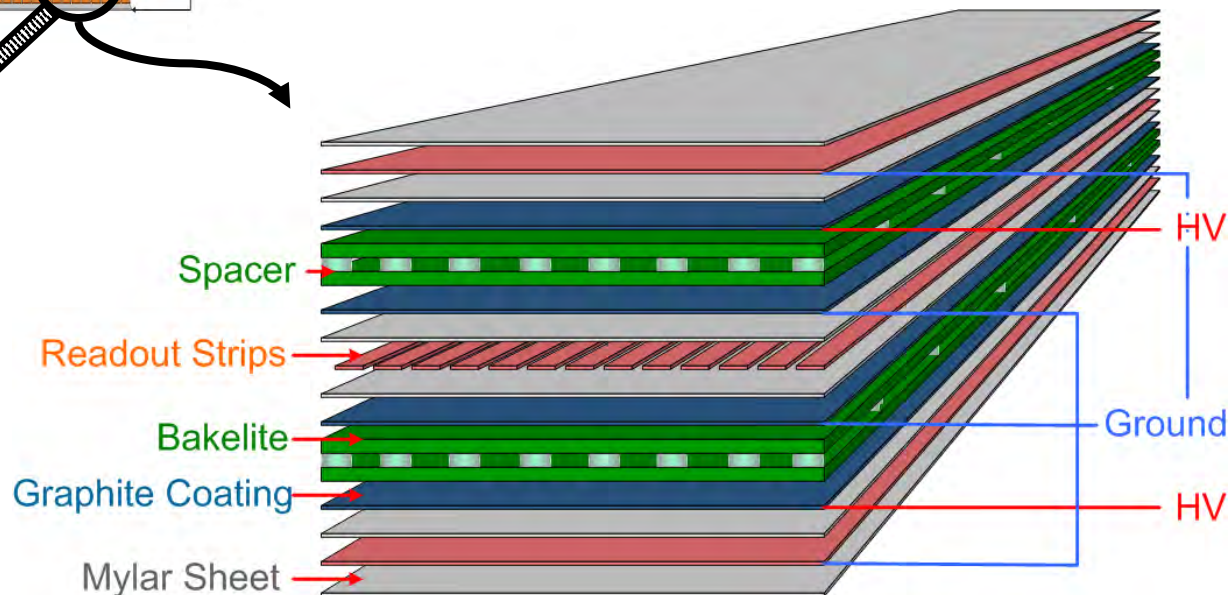
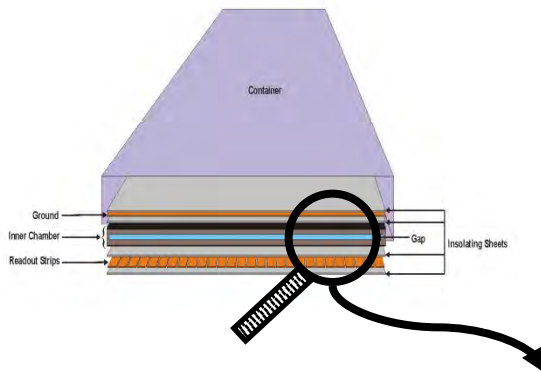


RPC aging	Remediation
Uncured Linseed oil formed droplets and stalagmites in the gap.	Use thinner Linseed oil coating and thoroughly polymerize the oil film before apply HV; Better surface Bakelite, completely abandon the use of Linseed oil coating.
Vanished graphite coating on the bakelite electrodes after accumulated certain amount of charge through the Bakelite.	Better technology for making the graphite coating; Switch to the avalanche mode operation.
Resistivity increase of the Bakelite electrode with the total accumulated charge.	Add water vapor into the gas mix; Switch to the avalanche mode operation.

CMS (CERN LHC): barrel/endcap trigger

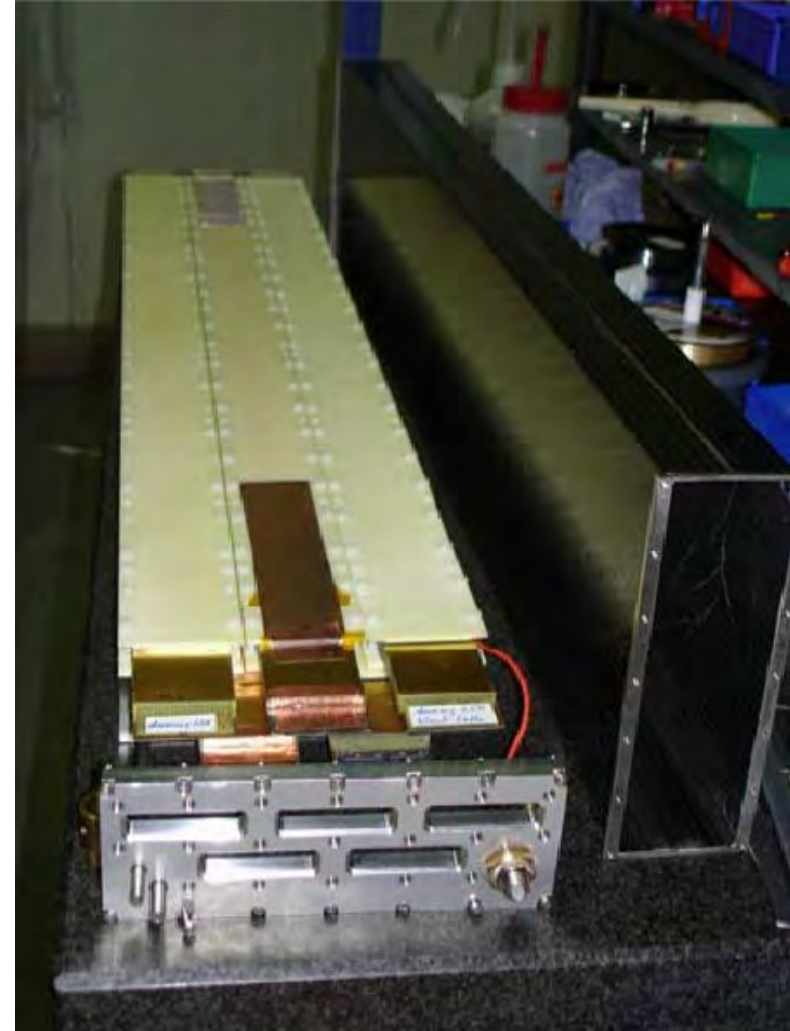
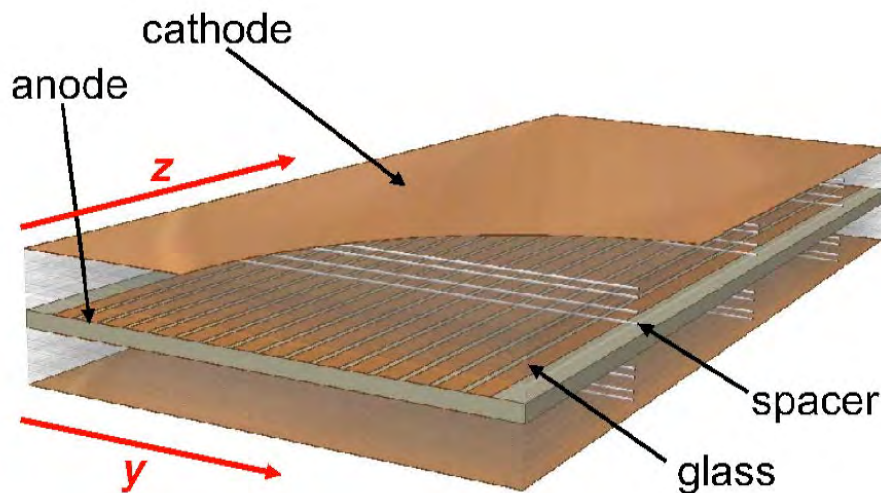
- Freon ($C_2H_2F_4$)/i- C_4H_{10} /SF₆ (95.5/3.5/0.3)
+ 5000 ppm H₂O
- Gap: 2 mm
- $U=9000$ V
- Total area: 2700 m², 105000 channels
- Time resolution < 3 ns

Single Gap RPC



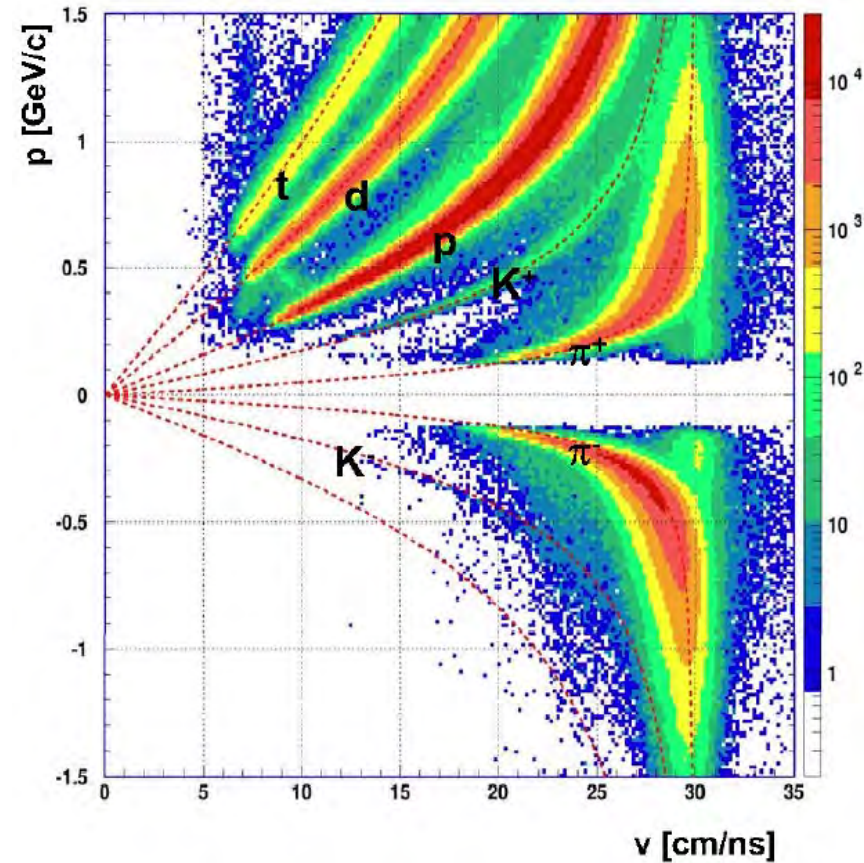
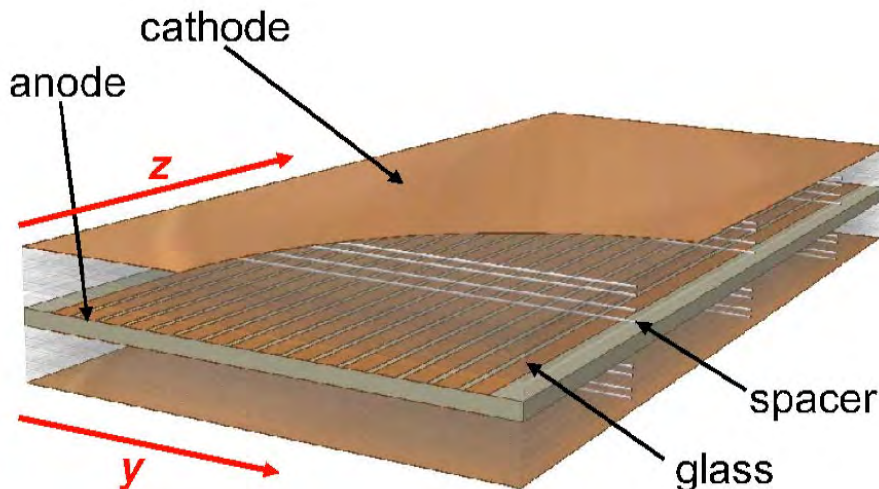
Multi-strip Multi-gap RPC:

- Active area: $90 \times 4.6 \text{ cm}^2$
- Gaps: $8 \times 220 \mu\text{m}$
- Strips: 16, 2-sided readout
- HV: 9.6 kV
- Gas: $\text{C}_2\text{H}_2\text{F}_4 / i\text{-C}_4\text{H}_{10} / \text{SF}_6$ (80/5/15)
- Resolution: $\sigma_{\text{RPC}} < 65 \text{ ps}$



Multi-strip Multi-gap RPC:

- Active area: $90 \times 4.6 \text{ cm}^2$
- Gaps: $8 \times 220 \text{ }\mu\text{m}$
- Strips: 16, 2-sided readout
- HV: 9.6 kV
- Gas: $\text{C}_2\text{H}_2\text{F}_4 / i\text{-C}_4\text{H}_{10} / \text{SF}_6$ (80/5/15)
- Resolution: $\sigma_{\text{RPC}} < 65 \text{ ps}$



4 Position Measurement

4.1 Resistive Plate Chambers

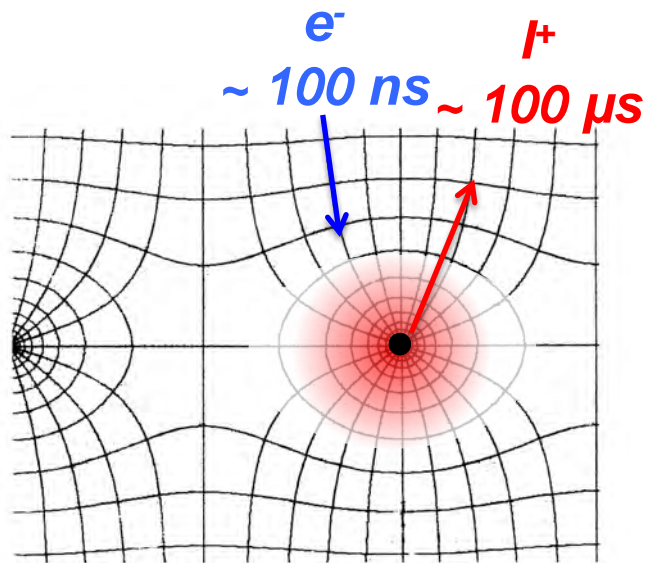
4.2 Micropattern Gaseous Detectors

4.3 Semiconductor Detectors

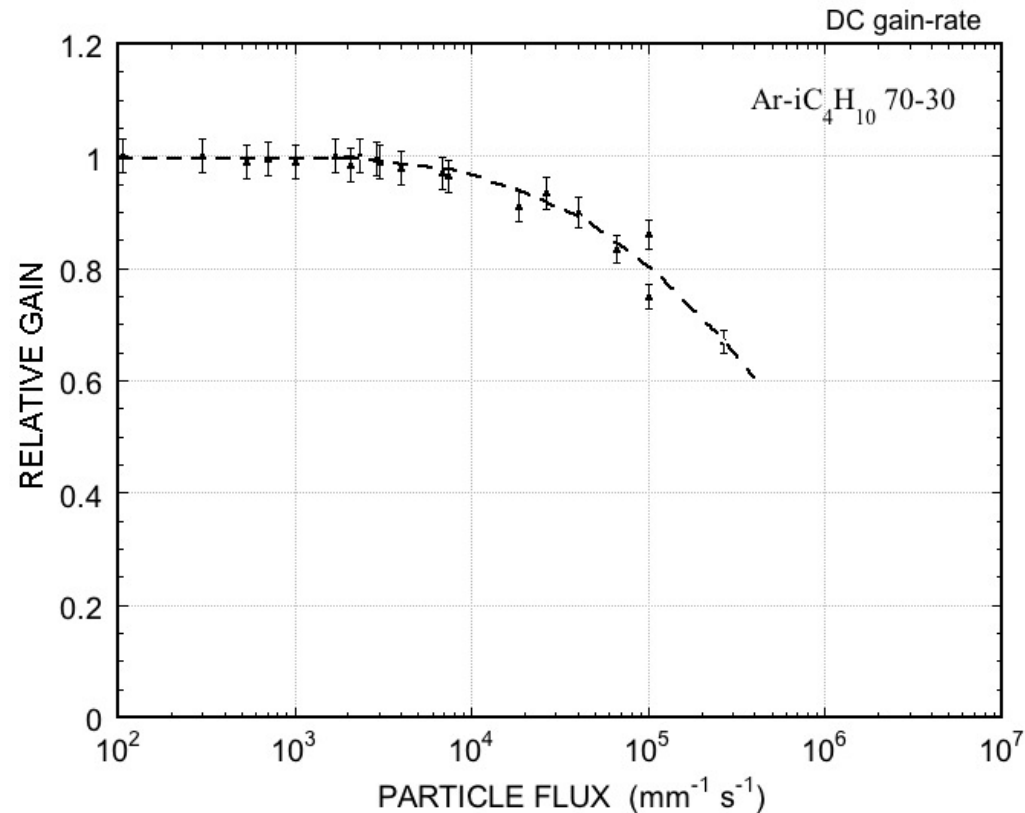
4.4 Track Reconstruction



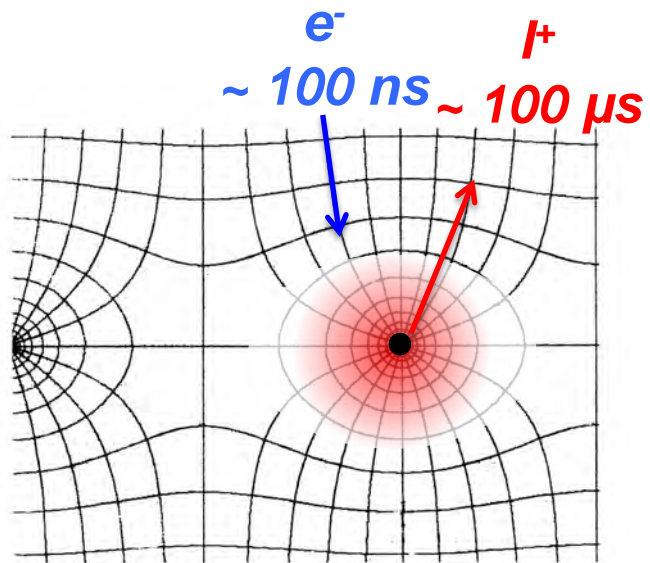
- Localization accuracy: typ. 100-500 μm
- Volume / 2-track resolution: typ. $10 \times 10 \times 10 \text{ mm}^3$ (signal induction on pads)
- Rate capability: limited by build-up of positive space-charge around anode



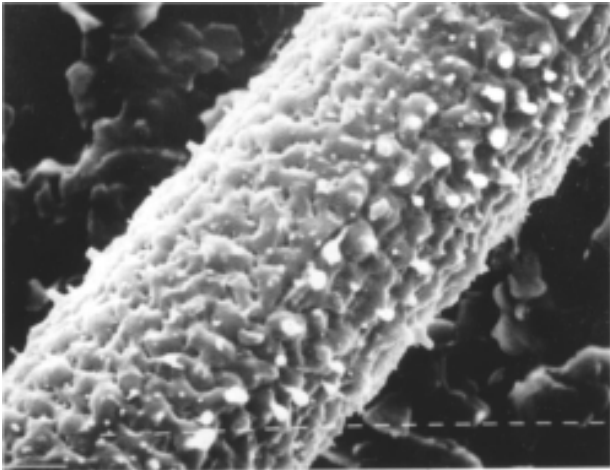
[A. Breskin et al., NIM 124, 189 (1974)]



- Localization accuracy: typ. 100-500 μm
- Volume / 2-track resolution: typ. $10 \times 10 \times 10 \text{ mm}^3$ (signal induction on pads)
- Rate capability: limited by build-up of positive space-charge around anode
- Ion backflow: $IB = I_{\text{cathode}} / I_{\text{anode}} \sim 30\%$ for TPC with MWPC



- Localization accuracy: typ. 100-500 μm
- Volume / 2-track resolution: typ. $10 \times 10 \times 10 \text{ mm}^3$ (signal induction on pads)
- Rate capability: limited by build-up of positive space-charge around anode
- Ion backflow: $IB = I_{\text{cathode}} / I_{\text{anode}} \sim 30\%$ for TPC with MWPC
- Aging and discharge damage: polymerization of organic compounds



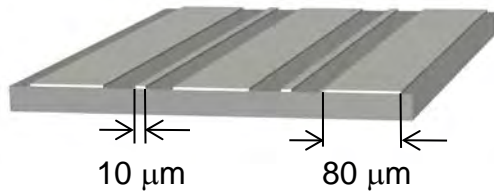
[O. Ullaland, LBL-21170, 107 (1986)]

⇒ Reduction of cell size
by a factor of 10

- Photolithography
- Etching
- Coating
- Wafer post-processing

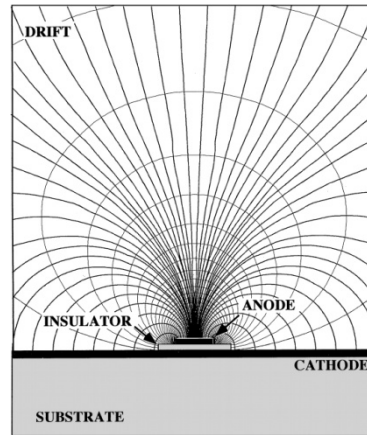
Microstrip Gas Chamber

[A. Oed, NIM A263, 351 (1988)]



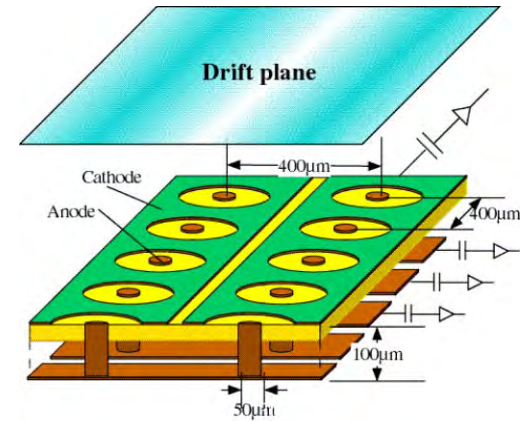
Microgap Chamber (MGC)

[F. Angelini et al., NIM A335, 69 (1993)]



Microdot Chamber

[S.F. Biagi et al., NIM A361, 72 (1995)]

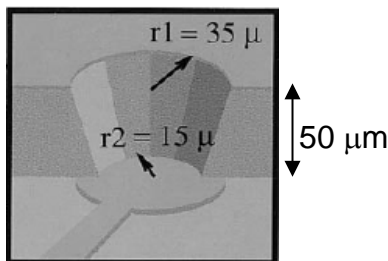


Compteur à Trous (CAT)

[F. Bartol et al., J. Phys. III 6, 337 (1996)]

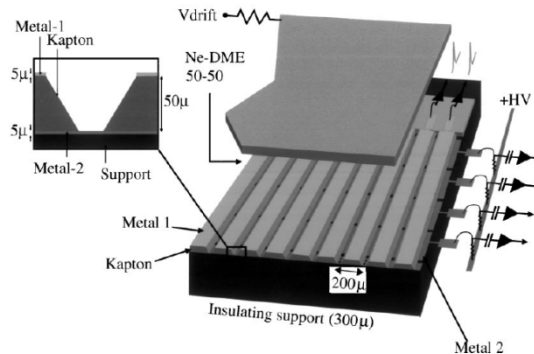
WELL Detector (μ CAT)

[R. Bellazzini et al., NIM A423, 125 (1999)]



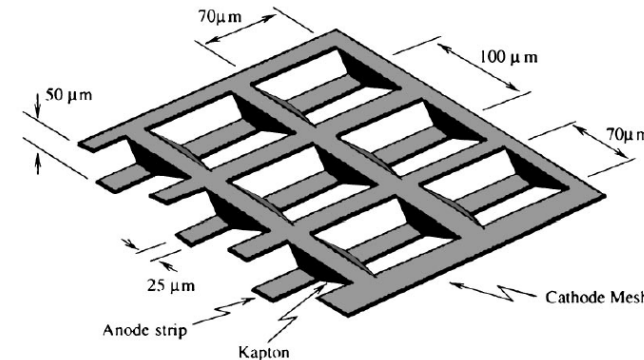
Micro Groove Counter

[Bellazzini et al., NIM A424, 444 (1999)]

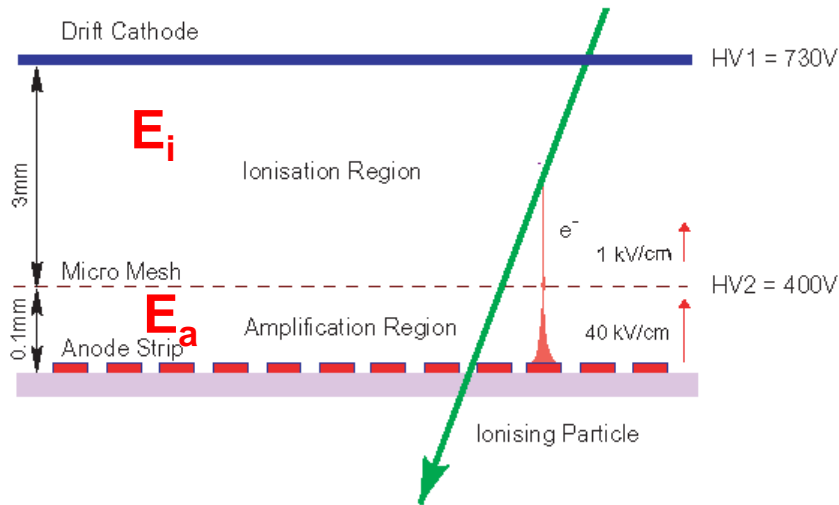


Micro Wire Detector

[B. Adeva et al., NIM A435, 402 (1999)]



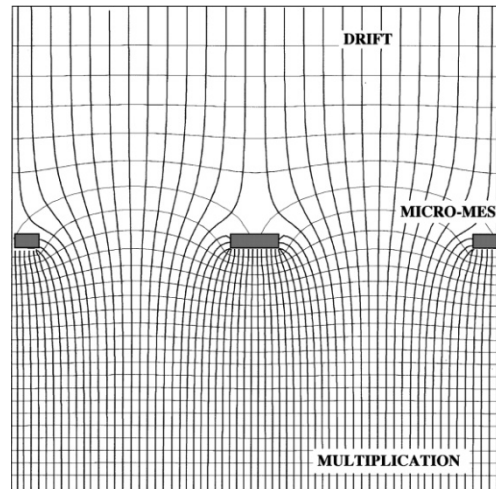
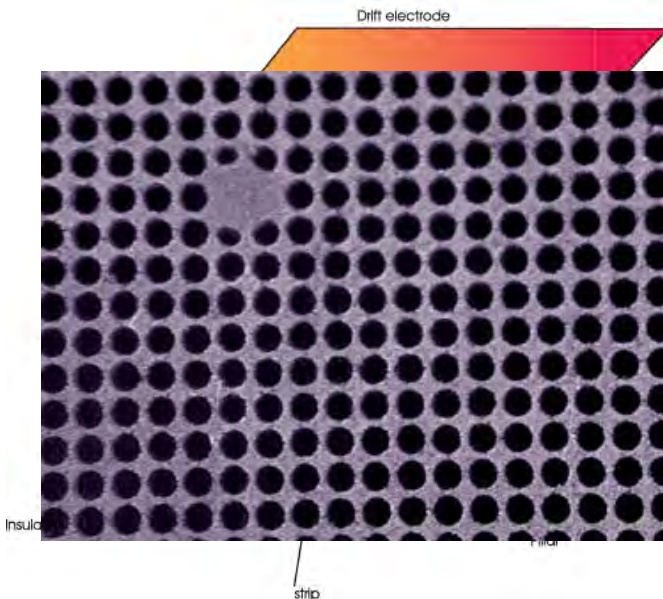
and many more...



Micromesh Gaseous Structure

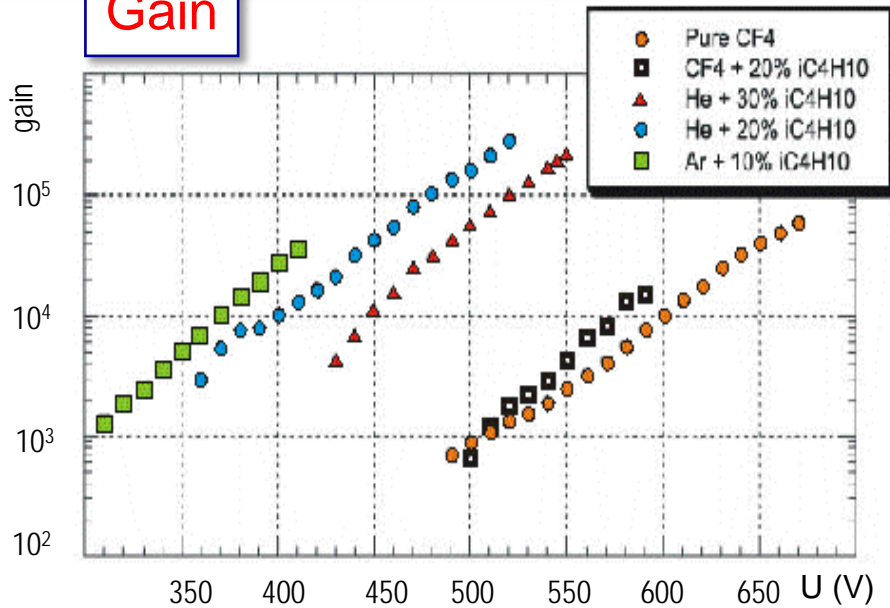
[I. Giomataris et al., NIM A376, 29 (1996)]

- Thin gap parallel plate structure
- Fine metal grid (Ni, Cu) separates conversion (~ 3 mm) and amplification gap (50-100 μm)
- Very asymmetric field configuration: 1 kV/cm vs. 50 kV/cm

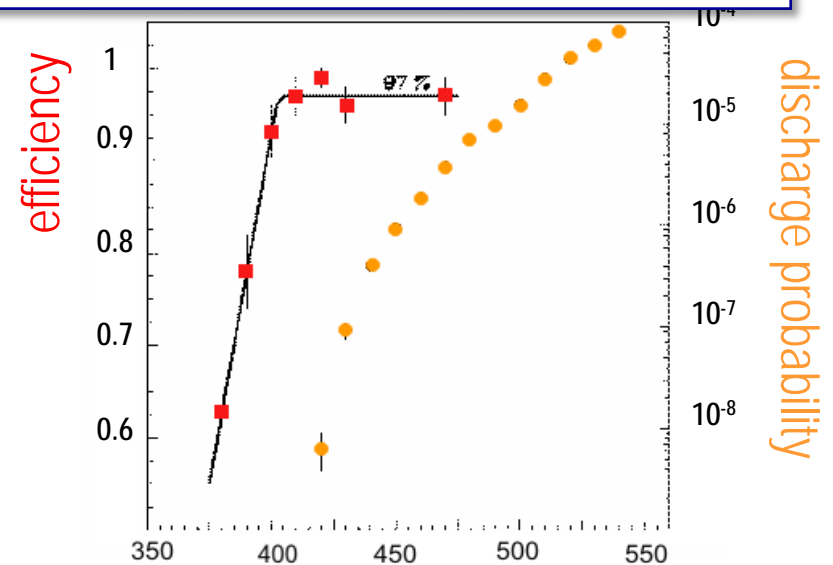


- ➔ Fast collection of ions (~ 100 ns)
- ➔ Saturation of Townsend coefficient (mechanical tolerances)
- ➔ good energy resolution

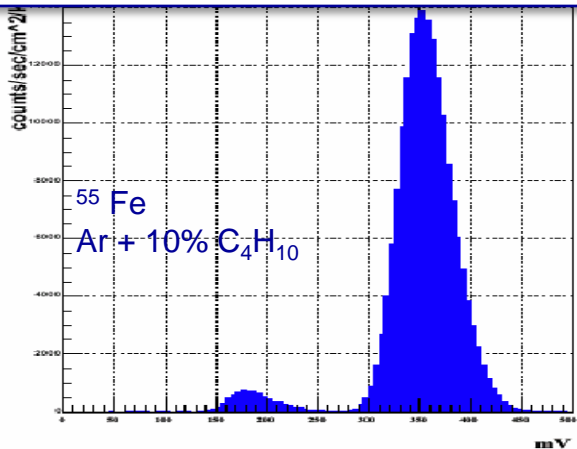
Gain



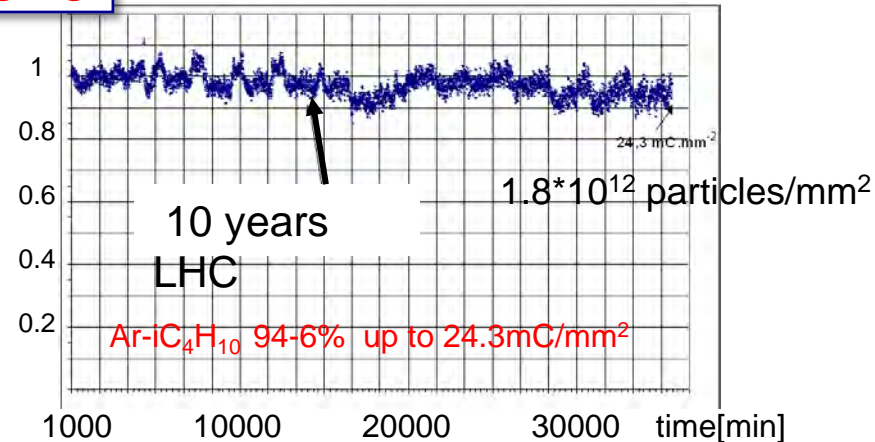
Efficiency & discharge probability

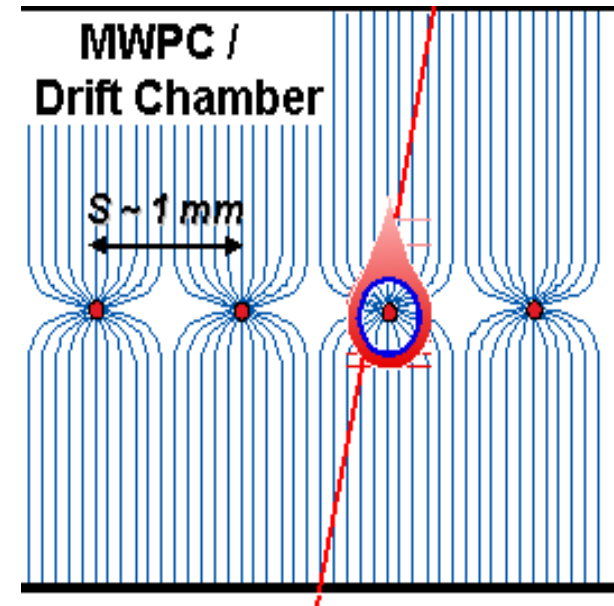
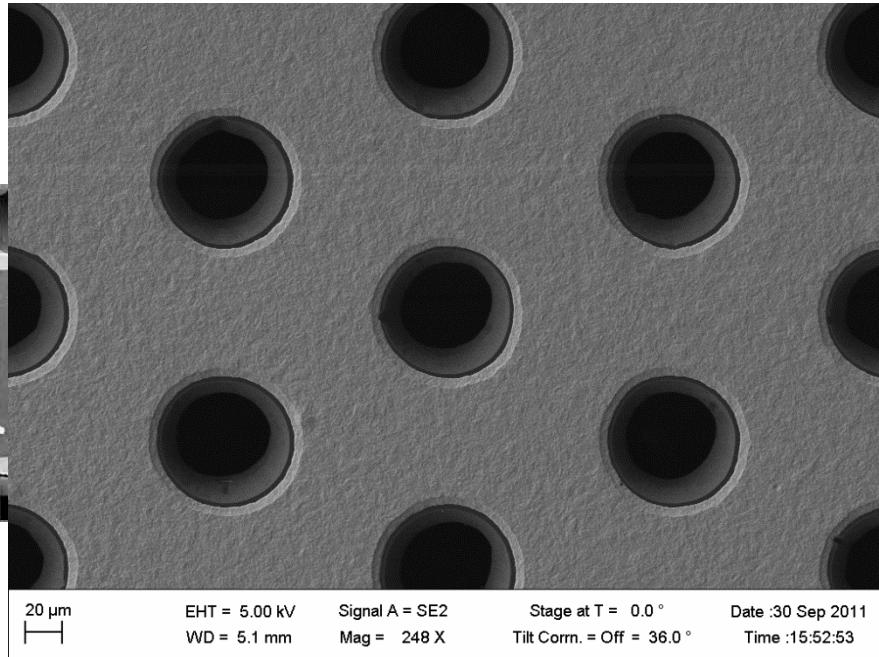


Energy resolution ~ 10%



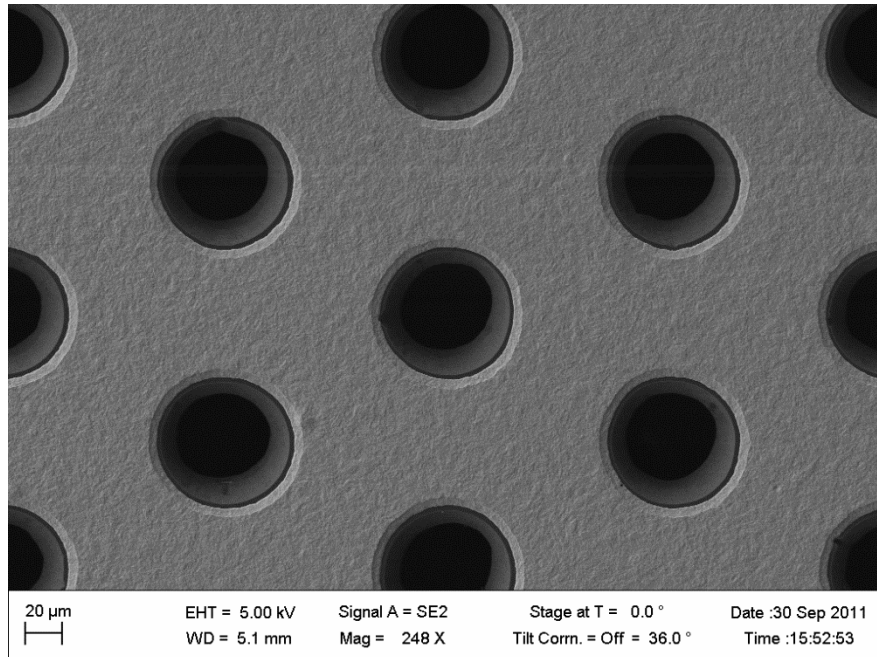
Aging





- GEM: **G**as **E**lectron **M**ultiplier
[F. Sauli, NIM A386, 531 (1997)]
- Thin **polyimide** foil, typ. 50 μm
- **Cu-clad** on both sides, typ. 5 μm
- Photolithography: $\sim 10^4$ holes/ cm^2
- **Granularity** 10x higher than MWPC

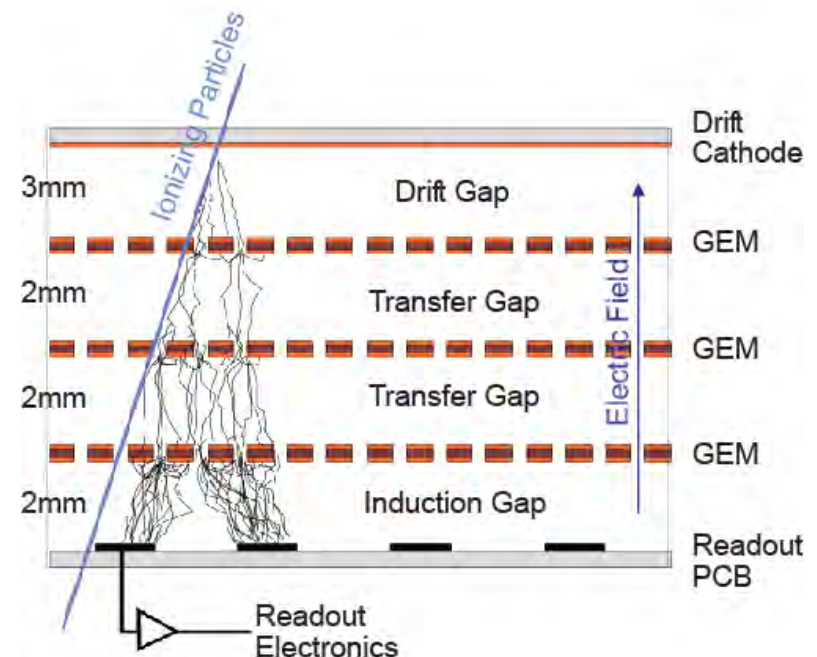
- $\Delta U = 300\text{-}500 \text{ V}$
 \Rightarrow high E-field: $\sim 50 \text{ kV/cm}$
 \Rightarrow avalanche multiplication



- **GEM: Gas Electron Multiplier**
[F. Sauli, NIM A386, 531 (1997)]
- Thin **polyimide** foil, typ. 50 μm
- **Cu-clad** on both sides, typ. 5 μm
- Photolithography: $\sim 10^4$ holes/ cm^2
- **Granularity** 10x higher than MWPC

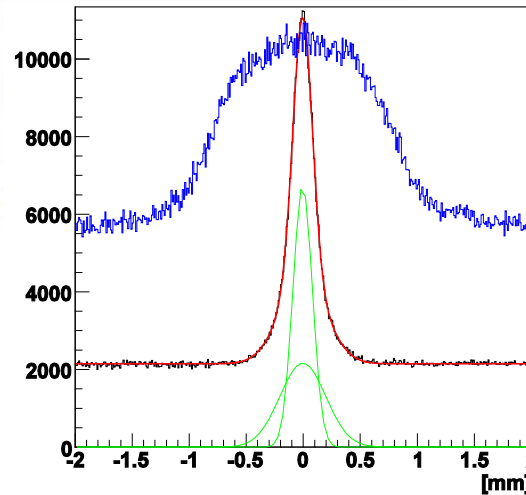
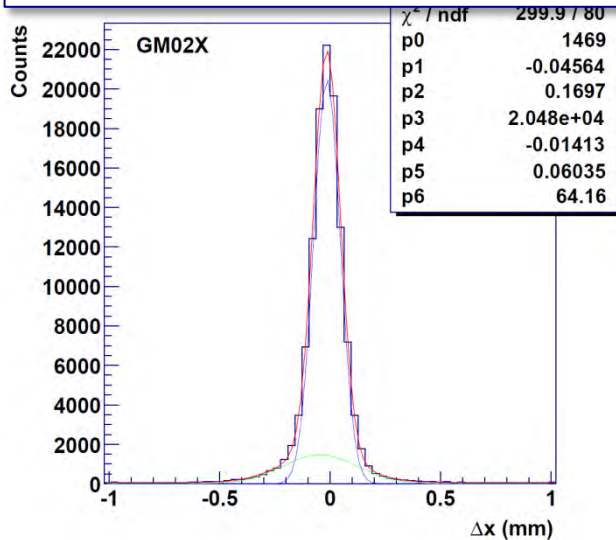
Triple GEM amplification

- ➔ higher gain at lower GEM voltages
[S. Bachmann, B. Ketzer et al., NIM A479, 294 (2001)]
- ➔ discharge prevention
[B. Ketzer et al., IEEE Trans. Nucl. Sci. 48, 1065 (2001)]
- ➔ no aging up to 7 mC/mm^2
[C. Altunbas, B. Ketzer et al., NIM A515, 249 (2003)]

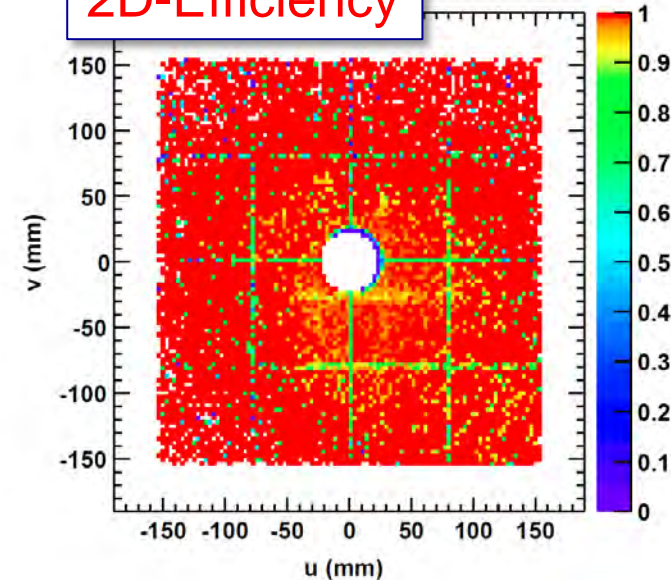


Spatial resolution: [B. Ketzer et al., NIM A535, 314 (2004)]

- low intensity: $50 \mu\text{m}$ (400 μm strips)
- $4 \cdot 10^7 \text{s}^{-1} \mu$: $70 \mu\text{m}$
- $2 \cdot 10^8 \text{s}^{-1} \mu$: $135 \mu\text{m}$ (1mm^2 pixels)



2D-Efficiency



Aging: [M Alfonsi et al., NIM A518, 106 (2004)]

- Ok up to 200mC/mm^2

